nagra.

Arbeitsbericht NAB 09-20

Borehole Gösgen KB5a: Mineralogy, Porosimetry and Pore Water Chemistry of the Effingen Member

December 2012

H. N. Waber, U. Mäder, M. Mazurek, M. Koroleva

Rock-Water Interaction,
Institut für Geologie, Univ. Bern

Nationale Genossenschaft für die Lagerung radioaktiver Abfälle

Hardstrasse 73
CH-5430 Wettingen
Telefon 056-437 11 11

www.nagra.ch

nagra.

Arbeitsbericht NAB 09-20

Borehole Gösgen KB5a: Mineralogy, Porosimetry and Pore Water Chemistry of the Effingen Member

December 2012

H. N. Waber, U. Mäder, M. Mazurek, M. Koroleva

Rock-Water Interaction,
Institut für Geologie, Univ. Bern

KEYWORDS

Effingen Member, Effinger Schichten, mineralogy, porosity, pore water, chloride, Groundwater

Nationale Genossenschaft
für die Lagerung
radioaktiver Abfälle

Hardstrasse 73
CH-5430 Wettingen
Telefon 056-437 11 11

www.nagra.ch

Table of Contents

List of Tables

List of Figures

1 Introduction

The Effingen Member (synonymous with Effinger Schichten) is one of the potential host rocks for the geological disposal for radioactive waste. First investigations of the Effingen Member date back to the Sediment Study performed by Nagra 25 years ago (Nagra 1988). More recently, the Effingen Member and surrounding lithologies have been investigated in more detail and applying most recent technologies in the EWS-borehole Oftringen (Waber 2008a).

Between October 2008 and January 2009 six cored (KB1, KB2, KB3, KB4, KB5 and KB5a) and one percussion-drilled (SB2) boreholes were drilled by KKG & Atel for various investigations on the site of the nuclear power plant Gösgen. The geological and stratigraphic description of the rock material recovered from these boreholes is given by Albert et al. (2009). In addition, mineralogical, chemical and physical properties of the encountered limestones to calcareous marls and their pore water could be performed on the core material of borehole KB5a. At the Gösgen site the rocks of the Effingen Member (Oxfordian) occur between about 66 and 307 m depth, are overlain by the Geissberg and Olten Members and underlain by the Birmenstorf Member, all of Oxfordian age. The Effingen Member occurs thus at shallower depth below the surface and at somewhat greater thickness compared to Oftringen (420 – 642 m depth) located some 8 km southwest of the Gösgen site.

Pore-water from low-permeability rocks cannot be sampled by conventional groundwater techniques and has to be characterised indirectly based on originally saturated rock material. In case of the Gösgen borehole 2 samples could be conditioned on-site immediately after recovery in order to minimise artefacts induced by exposure to the atmosphere (e.g. evaporation, oxidation), and this constitutes a pre-requisite for a complete pore water characterisation. Further 10 samples were treated conventionally following about 4 months of storage under atmospheric conditions, which limited the pore water investigations for these samples. Indirect extraction methods deliver only partial information about the pore water composition and need to be supported by mineralogical and petrophysical data. By combining the results of different experimental and modelling techniques a pore-water composition might then be derived. The plausibility of the derived composition is assessed by comparing the spatial distribution of pore-water compositions with that of groundwater in over- and underlying aquifers and the palaeo-hydrogeological evolution of the area.

The present report describes the mineralogical, petrophysical and geochemical investigations performed on drillcore material obtained from borehole KB5a drilled at the Gösgen site. It should be noted that borehole KB5a was drilled only to about 156 m depth and samples for porewater investigations are restricted to the upper half of the Effingen Member rocks. Supporting data such as the geological and hydrogeological description are given in Albert et al. (2009) and Enachescu et al. (2010).

2 Hydrogeological Setting

The Gösgen boreholes are located in the north-western Molasse basin, close to the thrust of the Folded Jura (Fig. 2-1). Borehole KB5a penetrated directly into the Oxfordian sediment sequence (Malm) below an about 30 m thick Quaternary overburden (Fig. 2-2). This contrasts with the profile encountered by the Oftringen borehole where below the Quaternary overburden about 360 m of Lower Freshwater Molasse and a thin Eocene shale layer (Boluston) overlay the Malm sediments (Albert & Bläsi 2008). The Oxfordian sediments encountered by the Gösgen borehole KB5A include coral-reef type limestone from the Olten Member (Balsthal Formation) down to 58.3 m, micritic limestone from the Geissberg Member (Villigen Formation) down to 67 m followed by silty to sandy marls with intercalated limestone layers of the Effingen Member (Wildegg Formation) down to the end of the borehole at 156 m depth (Albert et al. 2009). In borehole KB5a no groundwater occurrence was detected and no hydraulic tests were performed.

The same sedimentary sequence was also penetrated by the neighbouring borehole SB2 that was drilled to a depth of about 350 m by destructive drilling and where hydraulic tests were conducted. In this borehole the fresh water head in the Effingen Member rocks is sub-hydrostatic and the hydraulic conductivity in this sequence is below 1.7×10^{-12} m/s (Fig. 2-2; Enachescu et al. 2010). At Gösgen a lower hydraulic conductivity is observed for the Effingen Member at shallow depth compared to the occurrence of the same unit at greater depth in the Oftringen borehole ($K < 1.3 \times 10^{-11}$ m/s; Fisch et al. 2008). Furthermore, the low hydraulic conductivity in the Effingen Member at shallow depth as recorded in the Gösgen borehole SB2 also contrasts with earlier observations where an enhanced permeability has been observed in the Effingen Member at depths of less than 200 m (Nagra 2008, Fig. 4.3-17).

Below the Effingen Member rocks the hydraulic conductivity increases to values of $0.33 – 1.7 \times 10^{-9}$ m/s in the test interval from 316.9 – 347.0 m (Enachescu et al. 2010), which includes the rocks of the Birmenstorf Member (Oxfordian) and the Varians-Schichten and Hauptrogenstein Formation of Dogger age. From this interval groundwater could be sampled under artesian conditions (Appendix A).

The upper boundary of the low-permeability sequence encountered by the Gösgen borehole KB5a could correspond to the contact with the Quaternary overburden made of fine- to coarse-grained gravel in a sandy matrix. Occurrences of groundwater can, however, not be excluded in the underlying coral-reef type limestone of the Olten Member and calcareous arenite of the Geissberg Member, but this cannot be confirmed given the absence of hydraulic tests at this level in borehole SB2 (Fig. 2-2). Because neither detailed hydraulic nor hydrochemical data are available, the upper boundary of the low-permeability sequence is not well defined.

The lower boundary of the low-permeable Effingen Member rocks is given by the groundwater sampled from the interval 316.9 – 347.0 m depth. The exact groundwater inflow point is unknown. Presumably it is located in the biodetritic limestone of the Varians-Schichten and/or the oolitic limestone of the Hauptrogenstein Formation, the latter being known as a heterogeneous, local aquifer in this area. At Oftringen, however, these lithologies do not produce groundwater.

The groundwater sampled from the depth interval 316.9 – 347.0 m is of a normal Na-(Ca)-Mg-Cl chemical type with about 10.5 g/L total dissolved solids and a Cl^- concentration of 5640 mg/L. At a corrected pH of 6.9 (measured 7.1), the groundwater is saturated with respect to calcite, dolomite, quartz, close to saturation with respect to celestite (SI = -0.13) and fluorite (SI = -0.14) and undersaturated with respect to gypsum (SI = -0.85) and strontianite (SI -0.51).

It has $\delta^{18}O$ and $\delta^{2}H$ values enriched in the heavy isotopes (-5.63 ‰ and -51 ‰) compared to present-day infiltration, a low ^{3}H activity near detection (0.8 ± 0.56 TU) and low ^{14}C of 6.58 ± 0.16 pmc. All this data combined suggests a long residence time for this groundwater. However, the considerable influence of water-rock interaction processes (carbonate-mineral reactions and cation exchange) does not allow a straight-forward conversion of the ^{14}C activity into a residence time.

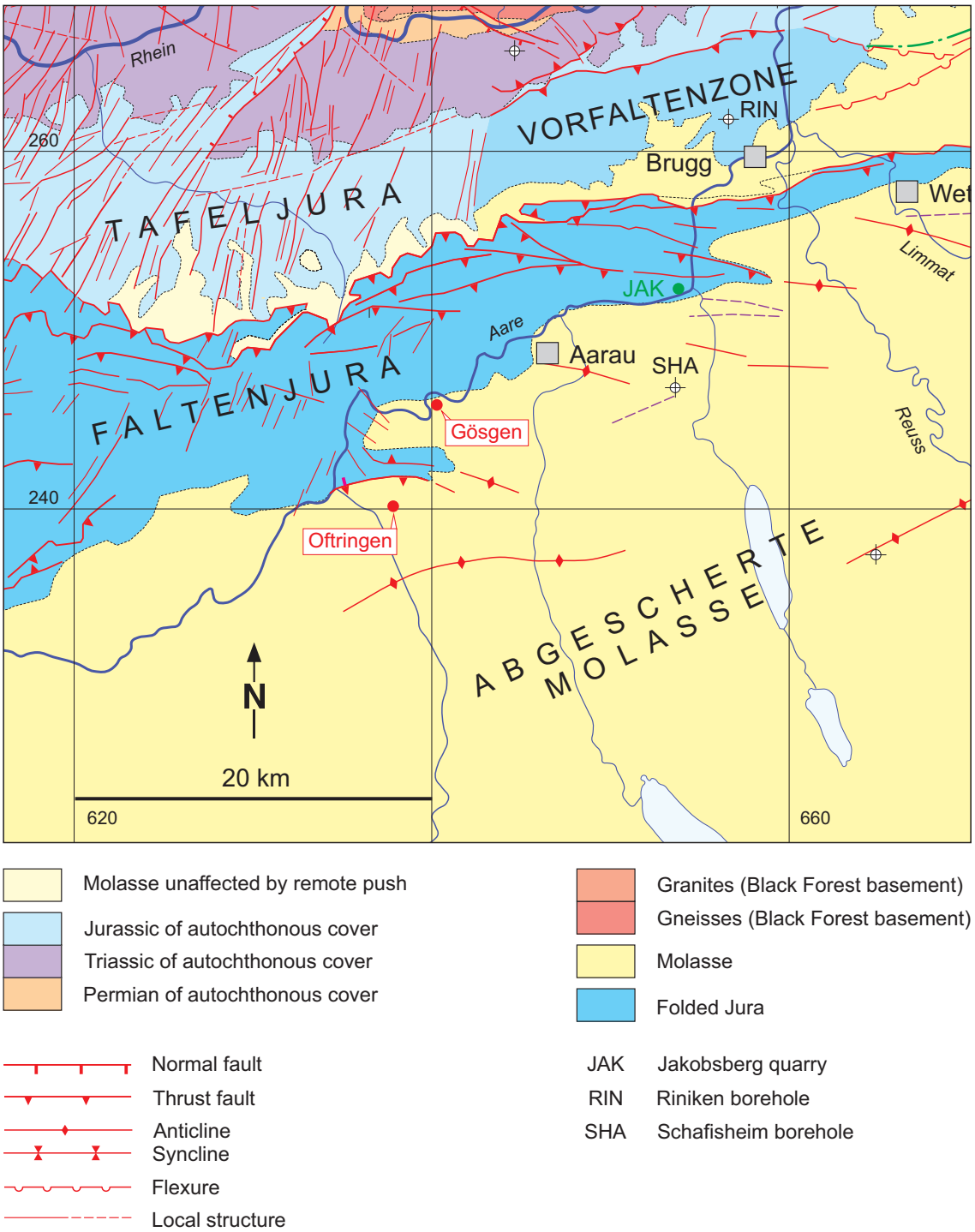

Fig. 2-1: Geological map of the vicinity of Gösgen and Oftringen (after Müller et al. 2002, Laws & Deplazes 2007).

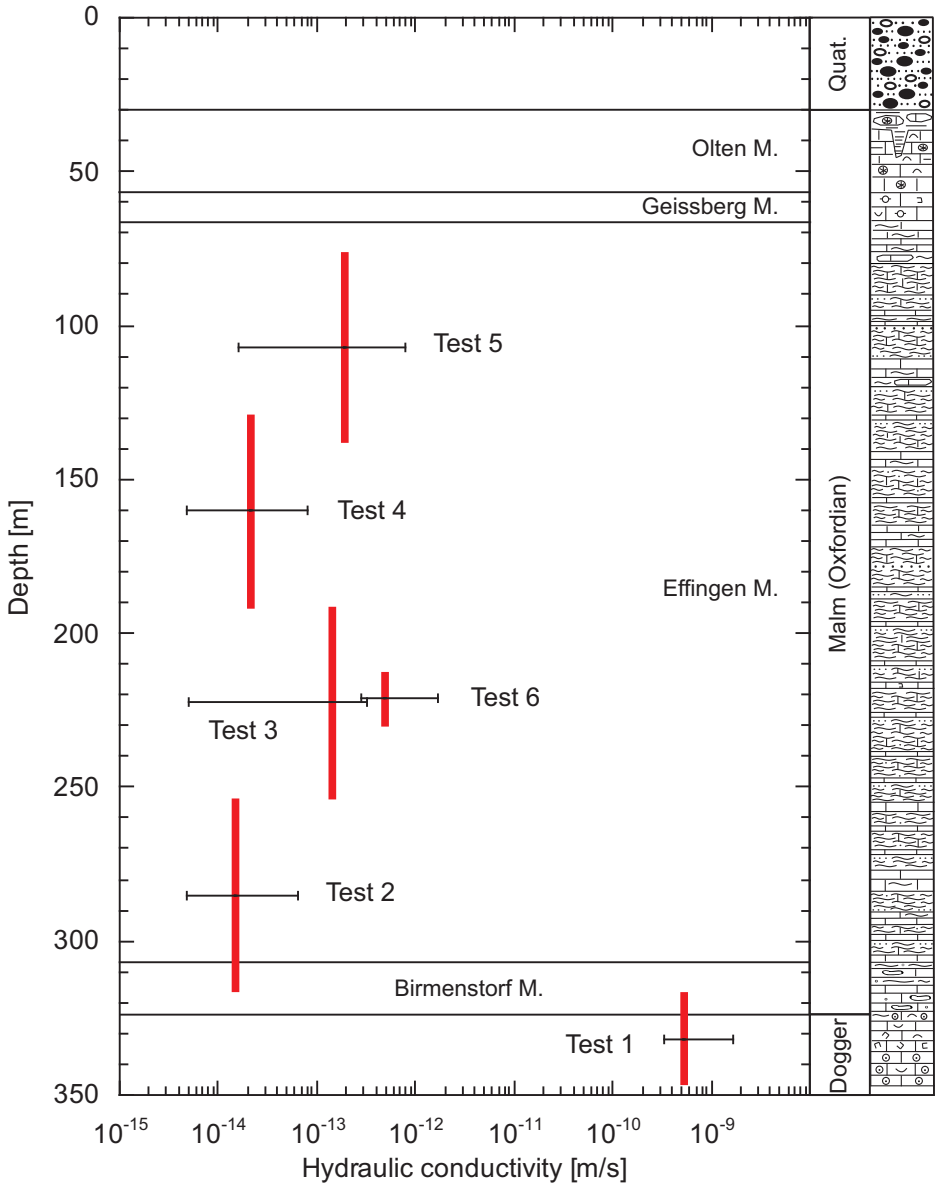

Fig. 2-2: Hydrologic conductivity profile (from Enachescu et al. 2010) and geology profile (from Albert et al. 2009) of the Gösgen borehole SB2 drilled some metres from borehole KB5a.

3 Materials and Methods

In borehole KB5a drilled at the Gösgen site the sampling programme for the mineralogical, petro-physical and geochemical investigations of the rocks and their relevant pore water included 12 intact drillcore samples between about 50 m and 150 m of borehole length, i.e. includes the upper half of the Effingen Member. A total number of 10 samples were collected from the Effingen Member, and 2 samples come from the overlying Geissberg and Olten Members, respectively.

Most analytical work was conducted at the Institute of Geological Sciences, University of Bern and if not stated otherwise the analyses were performed at this institution.

3.1 Sampling and sample conditioning

For legibility reasons the sample labelling adopted in this report is a subsequent numbering of the samples with depth using the "GOS" as prefix, and similar labelling was used for the laboratory studies. The conversion of this sample description to the Nagra sample number and the depth along borehole (borehole length) and the analytical program performed on the rock samples and experiment solutions are given in Table 3-1.

The immediate protection of the rock samples from evaporation, degassing and oxidation is an important requirement when investigating pore water of low-permeability rocks. In the present case the necessary on-site conditioning (i.e. vacuum packing) was only applied to 2 out of 12 samples. All other samples were stored under atmospheric conditions for about 4 months before they were transferred to the laboratory. All samples were prepared between 2-4 weeks after reception in the laboratory. Preparation included the removal of the outermost 2 cm of the drillcore rim, drying of the 2 on-site conditioned samples under controlled N_2 atmosphere in the glovebox and grinding of the dry rock material. The sub-sample dedicated to the advective displacement experiment (GOS-8) was immediately vacuum-packed after dry-cutting the core into two pieces.

3.2 Mineralogical analyses

3.2.1 Whole rock mineralogy

The whole rock mineralogy of the rock samples was determined by X-ray diffractometry using a PHILIPS PW3710 diffractometer. Rock material from the rim of the drillcores was ground in a ring mill to a grain size of less than 2 µm, mounted on a sample holder, disorientated with a stamp, and scanned with a Cu Kα radiation from 2° to 70° 2θ angle. Quantification of the contents of quartz, feldspars and carbonates (calcite, dolomite, siderite) was performed by an internal standardisation utilising the diffraction peak-intensity ratio of the mineral to that of an internal LiF-standard. The relative error of such determinations is about ± 5 %.

For carbonate mineral content the relative contents of different carbonate minerals derived from the XRD peak intensities were corrected using the total inorganic carbon content measured by IR-spectroscopy (see section 3.3.3). The total sulphur concentrations measured by IR-spectroscopy were converted to pyrite content assuming that (observed) pyrite is the dominating sulphur-bearing mineral phase. The sum of sheet silicates present in the rock, which mainly consists of clay minerals, was calculated by the difference of 100 % minus the sum of all other phases.

Tab. 3-1: Analytical programme performed on drillcore samples collected from the Gösgen borehole KB5a.

Sample	Depth [m along bore-hole]	Strati-graphy	Mineralogy		Petrophysical Parameters					Geochemical & Pore Water Properties				
			Whole Rock	Clay Fraction	Gravi-metric Water Content	Bulk Density[2]	Grain Density	BET	Water Activity	Aqueous Extrac-tion[3]	Ni-en Extrac-tion (CEC)[4]	Advec-tive Displace-ment
GOS-1	50.12	Olten Member	×	×		×	×			×		
GOS-2	63.92	Geissberg Member	×	×		×	×			×		
GOS-3	72.77	Effingen M.	×	×		×	×	×		×		
GOS-4	83.21	Effingen M.	×	×		×	×	×		×		
GOS-5	92.85	Effingen M.	×	×		×	×	×		×		
GOS-6	103.04	Effingen M.	×	×		×	×	×		×		
GOS-7	117.38	Effingen M.	×	×		×	×	×		×		
GOS-8[1]	122.89	Effingen M.	×	×	×	×	×	×	×	×	×	×
GOS-9[1]	123.71	Effingen M.	×	×	×	×	×	×	×	×	×	
GOS-10	133.08	Effingen M.	×	×		×	×	×		×		
GOS-11	145.59	Effingen M.	×	×		×	×	×		×		
GOS-12	153.31	Effingen M.	×	×		×	×	×		×		

[1] Preservation of saturated state (on-site conditioning) and laboratory treatment under controlled conditions (glove-box).

[2] Bulk wet and dry density for samples GOS-8 and GOS-9; bulk dry density for all other samples.

[3] 4 solid:liquid ratios in glovebox, anion and cation concentrations for samples GOS-8 and GOS-9; 1 solid:liquid ratio under ambient conditions and anions only for all other samples.

[4] 4 solid:liquid ratios under controlled conditions (glovebox).

3.2.2 Inorganic carbon, organic carbon, and total sulphur of whole rock

The concentrations of total carbon (C_{tot}), inorganic carbon (C_{inorg}) and total sulphur (S_{tot}) were determined with a CS-Mat 5500 element analyzer (Ströhlein GmbH & Co, Germany). In this technique approximately 0.02 – 0.1 g of rock powder is heated to 1350 ° and 1550 °C in an O_2 or N_2 atmosphere, respectively, to liberate all volatile components.

Total carbon and sulphur are measured by IR (infrared) spectroscopy as CO_2 and SO_2 after oxidation in an O_2 atmosphere. Inorganic carbon (i.e. essentially from carbonate minerals) is measured separately in a N_2 atmosphere. The gas is passed through a Mg-perchlorate tube to remove water and then pumped through the CO_2 and SO_2 analysers. The peaks of CO_2 and SO_2 in the carrier gas are measured by IR-spectroscopy. Separate NDIR (non-dispersive infrared absorbance) analysers are used for each of the two species. Organic carbon (C_{org}) is calculated by difference of C_{tot} and C_{inorg}. The calibration is made with pure $CaCO_3$ for carbon and Ag_2SO_4 for sulphur. The detection limit is around 0.1 wt.-% for all three parameters (S_{tot}, C_{tot} and C_{inorg}).

3.2.3 Clay mineralogy

The clay mineralogy of the rock samples was determined by X-ray diffractometry using a PHILIPS PW1810 diffractometer. The clay fraction of less than 2 µm was separated by sedimentation in a 0.01N NH_4OH-solution column from grinded rock material of about 60 µm grain size. The clay fraction was removed from the supernatant suspension by centrifugation. Orientated samples were obtained by mounting the clay material on glass sample holders. For each rock sample three different preparations were prepared: i) dried under air, ii) saturated with ethylene glycol for the identification of expandable clay minerals, and iii) heated at 550 °C for one hour for the distinction between kaolinite and chlorite.

Scanning of the samples by X-ray diffractometry occurred at a velocity of 2° per minute from 2° to 40° 2θ angle using a Cu Kα radiation. The relative ratios of the individual clay mineral contents were determined by the peak-intensity ratios and taking the different X-ray absorption capacity of the individual clay minerals into account.

3.3 Petrophysical measurements

3.3.1 Gravimetric water content

The water content of the on-site conditioned samples GOS-8 and GOS-9 was obtained by the gravimetric determination of water loss by drying sample aliquots of approximately 160 – 370 g at 105 °C to constant weight. Duplicate measurements were performed for both samples. The absolute error of the weight determinations is ± 0.002 g. The gravimetric water content (WC_{wet}) was then calculated from the change in weight upon drying ($m_{wet} - m_{dry}$) and is expressed relative to the wet mass m_{wet} of the rock according to:

$$WC_{wet} = \frac{m_{wet} - m_{dry}}{m_{wet}} * 100\% \qquad (1)$$

3.3.2 Grain and bulk density

The grain density (ρ_g) was measured by kerosene-pycnometry in duplicate. The volume of the pycnometer was derived from the weight of kerosene that filled the pycnometer initially. The density of kerosene (ρ_k = 0.78 g/cm^3 at 20 °C) was checked using an aerometer. For the grain density measurement, powdered rock material was dried at 105 °C to constant weight. Approximately 15 g of the sample were placed in the pycnometer, which was subsequently filled with kerosene while continuously removing the air by a vacuum pump. The volume of kerosene, which was required to fill the pycnometer containing the rock material, was calculated from the weight of kerosene. The rock sample volume was computed as the difference between the volume of kerosene in the pycnometer with and without the rock material. The grain density then is obtained according to:

$$\rho_g = \frac{\rho_k * (m_{rock+pycn} - m_{pycn})}{m_{rock+pycn} - m_{pycn} + m_{k+pycn} - m_{rock+k+pycn}} \tag{2}$$

where $m_{rock+pycn}$ is the mass of the dry rock powder in the pycnometer, m_{pycn} is the mass of the pycnometer, m_{k+pycn} is the mass of the pycnometer filled with kerosene and $m_{rock+k+pycn}$ is the mass of the pycnometer with the rock sample and the kerosene.

The bulk wet density, $\rho_{b.wet}$, was measured in duplicate on the on-site conditioned samples GOS-8 and GOS-9 using the paraffin displacement method and following the Archimedes principle. Two homogeneous rock pieces (1.5 – 2 cm^3) were taken from the saturated centre of the drill-core. The sample volume was determined by weighing the rock sample in air and during immersion into paraffin (ρ_p = 0.86 g/cm^3 at 20 °C) using the density accessory kit of Mettler Toledo™. The bulk wet density is calculated according to:

$$\rho_{b.wet} = \frac{\rho_p * m_{rock+pw}}{m_{rock+pw} - m_{(rock+pw)P}} \tag{3}$$

where $m_{rock+pw}$ is the mass of the wet rock sample in air and $m_{(rock+pw)P}$ is mass of the wet rock sample in paraffin.

For samples GOS-8 and GOS-9 the bulk dry density ($\rho_{b.dry}$) is calculated from the water content relative to the dry mass of the rock and the bulk wet density according to:

$$\rho_{b.dry} = \frac{\rho_{b.wet}}{1 + WC_{dry}} \tag{4}$$

where

$$WC_{dry} = \frac{m_{wet} - m_{dry}}{m_{dry}} \tag{5}$$

with m_{wet} = wet mass of the rock and m_{dry} = dry mass of the rock.

The non-conditioned samples were first dried at 105 °C to constant weight and followed by bulk dry density measurements using the paraffin displacement method as described above for bulk wet density.

3.3.3 Physical porosity and water-loss porosity

The total or physical porosity, ϕ_{tot}, of a rock sample is the ratio of the pore volume to the total volume of the sample (V_{pores} / V_{tot}), where the total volume is the sum of the pore volume and the volume occupied by mineral grains (Norton & Knapp 1977). The total porosity (ϕ_{tot}) is calculated from the values of bulk dry density and grain density according to:

$$\phi_{tot} = 1 - \frac{\rho_{b.dry}}{\rho_g} \tag{6}$$

with $\rho_{b.dry}$ = bulk dry density and ρ_g = grain density.

The water-loss porosity or volumetric moisture content of a rock sample, ϕ_{WL}, expressed as a fraction of one, is the ratio of its water-filled pore volume to its total volume (V_{wat} / V_{tot}) and is obtained according to:

$$\phi_{WL} = \frac{WC_{wet} \cdot \rho_g}{WC_{wet} \cdot \rho_g + (1 - WC_{wet}) \cdot \rho_{wat}} \tag{7}$$

where ρ_{wat} = density of the pore water, ρ_g = grain density of the rock, and WC_{wet} = water content of the rock relative to its wet weight (*cf.* equation 3).

Initially, the density of pore water is unknown. Pore water investigations performed in the EWS-borehole Oftringen indicated that the salinity of the pore water in the deeper-seated rocks of the Effingen Member is less than that of seawater (Waber 2008a). This justifies the assumption of a pore-water density of 1.00 g/cm^3 for the two samples GOS-8 and GOS-9 from the Gösgen KB5a borehole. A salinity correction for the porosity calculations was thus ignored because such a low pore-water salinity does not affect the calculations beyond the analytical error.

3.3.4 Specific surface area (BET)

The specific surface area of powdered samples (grain size ≤ 2 mm) was determined by nitrogen adsorption isotherms at 150 °C using a Coulter SA 3100 surface analyzer. Powdered rock material was weighed to an accuracy of 0.001 grams and thoroughly desorbed of primary adsorbed gases under vacuum at 150 °C for approximately one hour before the measurement of the nitrogen adsorption isotherms. The N_2-surface area was calculated using the Brunauer, Emmet and Teller method (BET; Brunauer et al. 1938) for a pressure range of P / P_0 from 0 to 1. The specific surface area, expressed as m^2/g, is then calculated from the N_2-surface area and the sample weight.

3.3.5 Water activity

The water activity (a_w) was measured on originally saturated rock material of the on-site conditioned samples GOS-8 and GOS-9 from the relative humidity of the air surrounding the sample. Measurements were performed using a HygroPalm AW1 device with a resolution of $\pm 0.001a_w$ and an accuracy of $\pm 0.003a_w$ (AwQuick mode). The measurement was conducted immediately after unpacking and removing the rim material from the drillcore samples.

3.4 Cation exchange properties

The cation exchange properties of the rocks from the Effingen Member were approached be the nickel-ethylenediamine, Ni-en, method (see Baeyens & Bradbury 1994, Bradbury & Baeyens, 1997/98). This method is based on the premise that Ni as a strong sorbent will exclusively replace all exchangeable cations from the mineral surfaces into solution.

Immediately after unpacking the on-site conditioned drillcore GOS-8 and GOS-9 in the laboratory, about 2 cm of the outer rim of the core were removed using a chisel and hammer. The crushed material from the central part of the core was quickly transferred into an oxygen-free glovebox with a continuous N_2 gas stream to minimise oxidation of sulphide minerals in the rock (e.g. pyrite). All further sample preparation and handling (drying, leaching, filtration) was performed in this glovebox, except for pulping the crushed material to a grain size < 63 µm in a ring mill. The latter procedure occurred under semi-closed conditions in the laboratory and lasted about 15 – 20 minutes including the sample transfer in and out of the glovebox. Ni-en extractions were performed on the pulped material at four different solid:liquid (S:L) ratios. The amount of pulped rock material varied between about 4 – 30 g for the different S:L weight ratios of 0.1, 0.25, 0.5 and 1 (in units of g rock per g solution). Each sample was prepared, extracted and analysed in duplicate (sub-samples *a* and *b* in Tab. 6-1).

The Ni-en solution was prepared using degassed, oxygen- and CO_2-free water that was prepared in the glovebox by boiling and N_2 bubbling over 30 minutes. The pH of the Ni-en solution was buffered to 8.0 – 8.2 by adding HNO_3 Titrisol ™ solution. Each sample was shaken end-over-end for 7 days in a polypropylene tube in order to equilibrate the extract solution with the calcite *and* dolomite that are present in the rocks. After phase separation by centrifugation, the supernatant leach solution was removed using a syringe and was filtered to < 0.45 µm. Apart from pH, analyses included major cations (Na^+, K^+, Ca^{2+}, Mg^{2+} and Sr^{2+}) and nickel and were performed using atomic absorption spectrometry, AAS. The analytical error of these measurements is less than ± 5 % based on multiple measurements of standard solutions and the cumulative error of the entire procedure (i.e. extraction and analysis) is approximately 10 %.

The *cation exchange capacity* (CEC) is then derived from the Ni-consumption, i.e. the difference between the Ni concentration in the initial and the final extract solution. The derivation of the *in situ cation exchange populations,* the cation concentrations measured in the final Ni-en extract solutions require correction for contributions from the pore water and dissolution reaction (calcite, dolomite etc) that occur during the experiments. Under favourable conditions such correction can be done using the cation and anion concentrations measured in the aqueous extract solution and geochemical model calculations.

3.5 Aqueous extraction tests

For all samples aqueous extraction tests were performed on material from the central part of the drillcores, i.e. after removal of about 2 cm of the outer rim of the core using a chisel and hammer. For the on-site conditioned samples GOS-8 and GOS-9 this was done immediately

after unpacking and the crushed material was quickly transferred into an oxygen-free glovebox with a continuous N_2 gas stream to minimise oxidation of sulphide minerals in the rock (e.g. pyrite). All further preparation and handling of these two samples (drying, leaching, filtration, pH measurement and titration of the extract solution) was performed in this glovebox, except for grinding the crushed material to a grain size < 63 µm in a ring mill. The total exposure time to air was about 15 – 20 minutes for these samples. For all other samples further preparation and handling occurred under laboratory conditions.

Aqueous extraction tests were performed at four different solid:liquid (S:L) ratios for samples GOS-8 and GOS-9 and at a S:L ratio of 1 for all other samples. The amount of pulped rock material varied between about 4 g and 30 g for the different S:L weight ratios of 0.1, 0.25, 0.5 and 1 (in units of g rock per g solution). Each sample was prepared, extracted and analysed in duplicate (sub-samples *a* and *b* in Tabs. 7-1 and 7-2).

The pulped rock material was placed into polypropylene tubes filled with an equivalent mass of degassed, oxygen- and CO_2-free water that was prepared in the glovebox by boiling and N_2 bubbling over 30 minutes. Each suspension was shaken end-over-end for 24 hours in a polypropylene tube. After filtration using 0.45 µm millipore filters, the supernatant solutions were immediately analysed in the glovebox for pH and alkalinity (by titration). Major anions (Cl^-, Br^-, NO_3^-, F^-, SO_4^{2-}) and cations (Na^+, K^+, Ca^{2+}, Mg^{2+}, and Sr^{2+}) were later analysed in the remaining solutions by ion chromatography using a Metrohm 861 Compact IC-system. The error of the ion chromatographic analyses is ± 5 % based on multiple measurements of standard solutions.

3.6 Advective-displacement technique for pore water extraction

The pore water extraction technique by forced advective displacement with an artificial pore water aims at obtaining a true sample of pore water subject to relatively minor artefacts. The method hinges on the availability of a saturated core sample processed and stored protected from atmosphere, the presence of sufficient connected porosity, the absence of significant preferred flow paths, and the ability to induce a relatively homogeneous advective-dispersive displacement front between the injected artificial pore water and the displaced *in situ* pore water. Ideally, a number of subsequent small aliquots can be sampled with minor admixture of the artificial pore water. Passive tracer components contained in the artificial pore water serve as a monitor for the proportion of artificial pore water contained in the extracted pore water (e.g. Br^-, ^2H_2O). The method with applications to indurated claystones is summarized in Mäder et al. (2004) and described in detail by Mäder (2006) and Waber (2008a).

Details of the apparatus and sample preparation are described and illustrated in section 8. In short, a drill core segment is cut square and placed between adapters separated by porous discs. The sample is sealed against the confining medium by an inner layer of Teflon and an outer layer of rubber. The infiltration system guides the gas-pressurized artificial pore water to the surface of the core sample where it is distributed by a porous Teflon / titanium disc. Likewise, the pore water forced out of the core sample is collected by a porous disc and guided through PEEK capillary tubing to a sampling device. Small syringes connected by luer adapters to the capillary are used as containers that protect the sample from atmosphere.

The apparatus allows choosing from a wide range of physical conditions for a pore water extraction experiment. The lower practical limit of hydraulic conductivity for a core sample for the method to work is approximately 10^{-14} m/s. Only small sample aliquots (0.5 – 3 mL) are commonly sampled from low-permeability rocks. This is especially true when the flow-active

porosity is small and therefore a relatively fast breakthrough (with respect to total pore volume) of the injected artificial pore water is to be expected. Typical durations for extracting a few samples from low-permeability rocks are several weeks to months.

The analytical programme has to be tailored to the objectives of the experiment, the expected chemical composition, the tracers used in the artificial pore water, and to the possibly very small sample size (e.g. Mäder 2006).

The method also offers the possibility to perform in-line measurements of electrochemical parameters such as pH, Eh, and electric conductivity by means of micro electrode flow-through cells. Only conductivity was continuously monitored for this experiment, and pH was measured in-line during two time intervals.

The hydraulic conductivity K [m/s] of the sample can be calculated for each sampling interval from the average volumetric flow rate Q [m^3/s], the sample length l [m] and cross section A [m^2], and the average difference in hydraulic head h [m_{H2O}] applied during displacement:

$$K = \frac{Ql}{Ah} \tag{8}$$

Sample GOS-8 (122.89 m borehole depth, Effingen Member, sandy-argillaceous limestone) was used for this pore water extraction. Accurate cutting of the core was relatively easy due to the excellent core quality.

The cut core was placed between titanium adapters separated by porous Teflon discs of 1 mm thickness. An insert of a porous titanium disc with 50 mm diameter and 1 mm thickness was fit into the centre of the Teflon disc to prevent a collapse of the porous Teflon when applying large pressures.

The artificial pore water was infiltrated from a Teflon-coated stainless steel sampling cylinder pressurized by helium. PEEK capillary tubing of 1/16" outer diameter was used, as well as a PEEK injection valve. An infiltration pressure of 56 bars (initial) and a hydraulic confining pressure of 72 bars were applied. The experiment was carried out at ambient temperature.

The sample aliquots were stored in the syringes as-is in a refrigerator. Samples were analysed for major cations and anions by ion chromatography in-house. Alkalinity was measured by titration only on selected samples. The experiment was terminated after 430 days. More details are provided in section 8.

4 Rock Mineralogy

The Gösgen borehole KB5a ends at 156 m below surface about in the middle of the Effingen Member, as shown by the neighbouring borehole SB2, which penetrated the entire Effingen Member unit between 66 and 307 m depth below surface (Albert et al. 2009). Rock samples investigated for pore water geochemistry from the borehole KB5a originate from the stratigraphic units of the Olten Member (1), the Geissberg Member (1) and the Effingen Member (10). It should be noted that the collected samples are not representative for the individual stratigraphic units, but are biased towards the more clay-rich layers of these units. A comprehensive stratigraphic and mineralogic description of the Gösgen borehole KB5a is given by Albert et al. (2009).

4.1 Whole-rock mineralogical composition

The rock samples of the Olten and Geissberg Member comprise pure limestone with more than 90 wt.-% calcite and less than 10 wt.-% clay minerals (Table 4-1). The rock samples of the Effingen Member have calcite contents between 32 and 85 wt.-% and compare with those of the Oftringen borehole (40 – 90 wt.-%). Dolomite and ankerite (3 – 14 wt.-%) are also present in similar amounts as in the Oftringen borehole, but display a more irregular distribution with depth (Tab. 4-1). With quartz and sheet silicate contents of 3 – 17 wt.-% and 10 – 34 wt.-%, respectively, the Effingen Member rock samples classify as argillaceous limestones to sandy-calcareous marls according to the Füchtbauer (1988; Fig. 4-1) nomenclature. Thus they describe the same lithologic variation as the Effingen Member rocks in the Oftringen borehole (*cf.* De Haller & Mazurek 2008).

Similar as at Oftringen, the total carbonate mineral content of the Effingen Member correlates negatively with the sheet silicate content whereas the latter is positively correlated with the quartz content (Fig. 4-2). The content of total sulphur in the rock is below 0.6 wt.-% in all samples except for the deepest one (GOS-12). No sulphur-bearing mineral phase other than pyrite was detected by X-ray diffractometry or by macroscopic inspection of the rocks. This does, however, not preclude the possible presence of trace amounts (< 1 wt.-%) of other sulphur-bearing minerals such as sulphates (e.g. celestite, anhydrite, gypsum). Assuming that all sulphur in the rock is associated with pyrite the total sulphur contents in the rocks convert to pyrite contents of less than 1 wt.-% for all but one sample (Tab. 4-1).

For all samples low contents of organic carbon are recorded with the highest values reaching 0.7 wt.-%. The organic carbon contents and the absence of a correlation with total sulphur contents (or pyrite, respectively) compare well with the Effingen Member rocks from the Oftringen borehole.

4.2 Clay mineralogy

Illite and illite-smectite mixed layers dominate the clay fraction (< 2 µm) present in the rocks from the Olten, Geissberg and Effingen Members in the Gösgen borehole KB5A (Tab. 4-2). Kaolinite is absent or present up to about 5 wt.-% in the rocks whereas chlorite and smectite occur only as traces if present at all.

Although only the upper half of the Effingen member was penetrated by the Gösgen borehole KB5A, some trends are indicated in the depth distribution of the clay mineralogy (Fig. 4-3): Kaolinite is absent in the upper part, but present in the lower part of the Effingen Member rocks and the illite-smectite mixed layer content decreases with depth.

The composition of the clay fraction of the Effingen Member at Gösgen shows some striking differences to that of the Effingen Member at Oftringen, although the total clay contents are similar for these rocks. Thus, the Effingen Member rocks at Gösgen have an illite to illite-smectite mixed layers ratio of 1.5 ± 0.4 (n = 10) compared to a ratio of 0.7 ± 0.2 (n = 19) in the clay fraction of the Oftringen samples (De Haller & Mazurek 2008). Furthermore, the rocks at Gösgen have about three times lower contents of kaolinite compared to the Oftringen rocks (2.4 wt.-% compared to 7.6 wt.-% in average) and smectite occurs only as traces. Based on the regional burial history an equivalent maturity would be expected for the Effingen Member at both sites and the difference in clay mineralogy is not yet well understood. Investigations about the maturity of organic materials would help to clarify this issue.

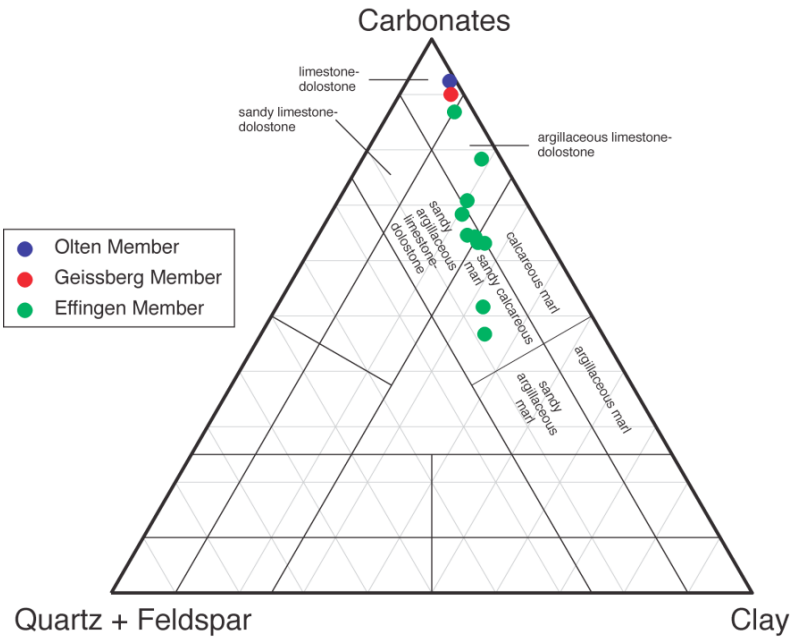

Fig. 4-1: Lithological classification of clastic sedimentary rocks after Füchtbauer (1988) for samples from the Gösgen borehole KB5a used for pore water investigations.

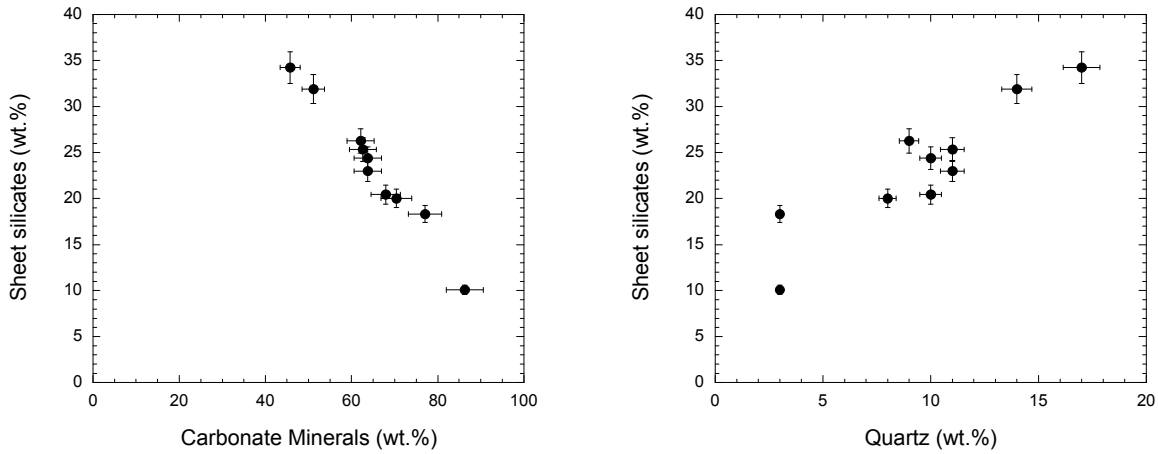

Fig. 4-2: Relationship between the contents of sheet silicates and total carbonate minerals (left) and quartz (right) in the 10 rock samples of the Effingen Member of the Gösgen borehole KB5a.

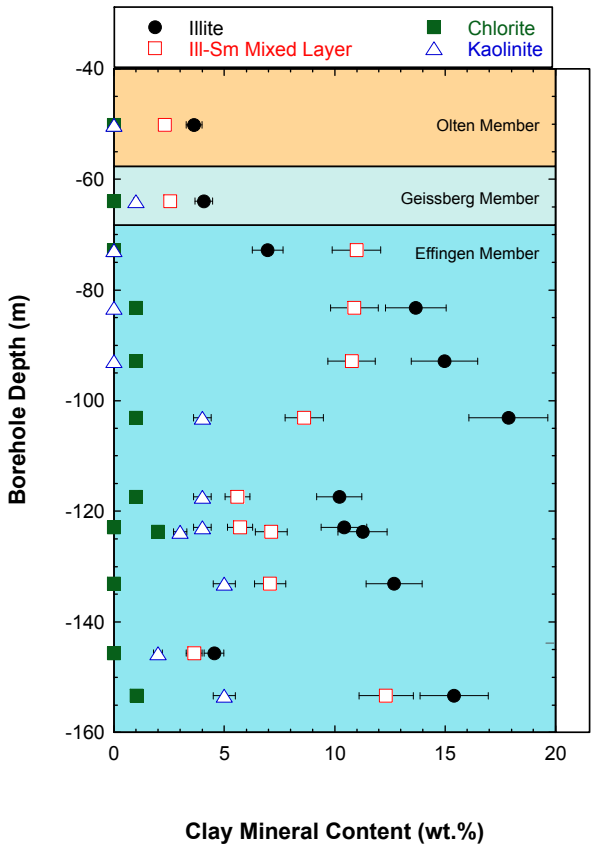

Fig. 4-3: Clay mineral composition of the whole rock versus borehole depth of the samples from the Gösgen borehole KB5a used for pore water investigations.

Individual clay mineral contents plotting at 0 wt.-% indicate trace amounts and contents below the detection limit of 1 % in the clay mineral diffraction patterns (*cf.* Tab. 4-3).

Tab. 4-1: Whole rock mineralogy based on XRD analysis and CS-Mat measurements of C_{inorg}, C_{tot} and S.

Sample	Depth [m along borehole]	Strati-graphy	Lithology	Calcite [wt.-%]	Dolomite /Ankerite [wt.-%]	Quartz [wt.-%]	Albite [wt.-%]	K-feld-spar [wt.-%]	Pyrite [wt.-%]	Sheet silicates [wt.-%]	C_{inorg} [wt.-%]	C_{org} [wt.-%]	S_{tot} [wt.-%]
GOS-1	50.12	OM	limestone	92	< 1	1	< 1	< 1	< 0.2	7	11.1	< 0.1	< 0.1
GOS-2	63.92	GM	limestone	90	< 1	2	< 1	< 1	< 0.2	8	10.8	0.2	< 0.1
GOS-3	72.77	EM	argill. limestone	74	3	3	< 1	< 1	0.9	18	9.3	0.7	0.5
GOS-4	83.21	EM	sandy-calc. marl	54	9	11	< 1	< 1	0.9	25	7.6	0.1	0.5
GOS-5	92.85	EM	sandy-calc. marl	59	3	9	< 1	1	0.9	26	7.5	0.7	0.5
GOS-6	103.04	EM	sandy-calc. marl	45	6	14	< 1	2	0.7	32	6.2	0.2	0.4
GOS-7	117.38	EM	argill. limestone	67	3	8	< 1	1	< 0.2	20	8.5	0.4	< 0.1
GOS-8	122.89	EM	sandy-argill. limestone	65	3	10	< 1	1	0.6	20	8.2	< 0.1	0.3
GOS-9	123.71	EM	sandy-argill. limestone	61	3	11	< 1	1	0.9	23	7.7	0.3	0.5
GOS-10	133.08	EM	sandy-argill. limestone	61	3	10	< 1	1	0.7	24	7.7	< 0.1	0.4
GOS-11	145.59	EM	argill. limestone	85	1	3	< 1	< 0.1	0.6	10	10.4	0.1	0.3
GOS-12	153.31	EM	sandy-calc. marl	32	14	17	< 1	1	1.9	34	5.6	0.1	1.0

OM: Olten Member, GM: Geissberg Member, EM: Effingen Member

Tab. 4-2: Clay mineralogy (fraction ≤ 2 µm) of the whole rock.

Sample	Depth [m along borehole]	Strati-graphy	Lithology	Illite	Ill-Sm ML	Smec-tite	Chlo-rite	Kaoli-nite
GOS-1	50.12	OM	limestone	4	2	1	trace	n.d.
GOS-2	63.92	GM	limestone	4	3	trace	trace	1
GOS-3	72.77	EM	argillaceous limestone	7	11	n.d.	trace	trace
GOS-4	83.21	EM	sandy-calcareous marl	14	11	n.d.	1	n.d.
GOS-5	92.85	EM	sandy-calcareous marl	15	11	n.d.	1	n.d.
GOS-6	103.04	EM	sandy-calcareous marl	18	9	n.d.	1	4
GOS-7	117.38	EM	argillaceous limestone	10	6	n.d.	1	4
GOS-8	122.89	EM	sandy-argill. limestone	10	6	n.d.	< 1	4
GOS-9	123.71	EM	sandy-argill. limestone	11	7	n.d.	2	3
GOS-10	133.08	EM	sandy-argill. limestone	13	7	n.d.	trace	5
GOS-11	145.59	EM	argillaceous limestone	5	4	n.d.	trace	2
GOS-12	153.31	EM	sandy-calcareous marl	15	12	n.d.	1	5

OM: Olten Member, GM: Geissberg Member, EM: Effingen Member; Ill-Sm ML: Illite-Smectite mixed layer
n.d. = not detected

5 Petrophysical Parameters

Petrophysical parameters whose determination requires saturated rock materials (water content, bulk wet density and water activity) could only be performed on the on-site conditioned samples GOS-8 and GOS-9. Petrophysical parameters that do not require saturated rock materials were obtained for the whole suite of samples. A compilation of all petrophysical data is given in Tab. 5-1.

5.1 Gravimetric water content

The water content relative to the wet mass of the rock (WC_{wet}) of samples GOS-8 and GOS-9 is 2.33 wt.-% and 2.53 wt.-%. The absolute difference in water content between duplicate samples is less than 0.19 wt.-%, suggesting limited heterogeneity of this rock property within duplicate samples. These water contents compare well with those of the Effingen Member from the Oftringen borehole (2.41 ± 0.88 wt.-%, Koroleva & Mazurek 2008) and also lie on the same trend line between water content and clay content.

5.2 Density and porosity

5.2.1 Grain and bulk density

The grain density ranges between 2.67 and 2.80 g/cm^3. Measured bulk dry density values range between 2.37 and 2.62 g/cm^3 and correlate negatively with the sheet silicate content of the rocks (Fig. 5-1), as already observed for the Effingen Member from the Oftringen borehole. Neither the grain density nor the bulk dry density display trends with depth.

The average bulk wet density measured on samples GOS-8 and GOS-9 is 2.60 g/cm^3 and 2.59 g/cm^3, respectively, and falls into the range obtained for the Effingen Member of the Oftringen borehole (2.56 – 2.67 g/cm^3, Koroleva & Mazurek 2008).

In the two samples where a direct comparison is possible, measured bulk dry density is 0.014 g/cm^3 (GOS-8) and 0.004 g/cm^3 (GOS-9) higher than that calculated from measurements of bulk wet density (note that only rounded data are given in Tab. 5-1). Similar observations were made for a suite of samples from Opalinus Clay at Mont Terri (Mazurek et al. 2010) where the difference was 0.1 g/cm^3, and also for clay-rich samples from Ordovician rocks of the Michigan Basin (Hobbs et al. 2010). In those two cases, physical porosities calculated using measured bulk dry densities were lower than water-loss porosities, which is not plausible. The likely explanation is that upon drying the clay-rich samples shrink and yield bulk-dry density measurements that are too high and do not represent in-situ conditions. Based on these recent findings, it is concluded that bulk dry densities based on measurements of bulk wet densities are in general more appropriate. In relation to Opalinus Clay and to the clay-rich samples from the Michigan Basin, samples GOS-8 and GOS-9 from the Effingen Member are relatively clay-poor, and so the discrepancy is of lesser importance.

Let us also note that most density measurements obtained for rocks from northern Switzerland to date relate to dry samples, meaning that they may overestimate the true values (and so under-estimate porosity). Once a larger data base of measurements of wet and dry pieces of the same samples becomes available, it may be possible to derive a correction algorithm, but this is not currently feasible.

5.2.2 Physical porosity and water-loss porosity

Physical porosities calculated from density measurements are listed in Table 5-1 and lie in the range 4.0 – 12.6 %. This large range is consistent with that observed for the Effingen Member in the Oftringen borehole (3.0 – 11.7 %, Koroleva & Mazurek 2008) and reflects the alternation between argillaceous, silty and calcareous lithologies. Physical porosity is positively correlated with the sum of sheet silicates, and to some degree also with the quartz content (Fig. 5-2). In contrast, a negative correlation is identified between the physical porosity and the total carbonate mineral content (Fig. 5-2).

For samples GOS-8 and GOS-9, physical porosity was calculated both using the measured bulk dry density and that derived from measured bulk wet density. The latter values are considered as more representative for in-situ conditions (see above) and are 0.2 – 0.5 % higher when compared to those based on measured bulk dry densities. It is concluded that for the relatively clay-poor rocks of the Effingen Member, the underestimation of physical porosity when using measured bulk dry density for the calculation is quantitatively of minor importance.

Water-loss porosity (ϕ_{wc}) calculated from water content and grain density according to equation (7) becomes 6.26 % and 6.71 % for samples GOS-8 and GOS-9. These values compare well with the average water-loss porosity of rocks with similar clay contents (20 – 30 wt.-%) from the Effingen Member of the Oftringen borehole (6.90 ± 1.18 %, Koroleva & Mazurek 2008).

The water-loss porosity of samples GOS-8 and GOS-9 is lower than the physical porosity by more than 2 % (Tab. 5-1). A slight difference of this kind can be explained by the fact that not all pore water is released from the rock by heating at 105 °C. However, the difference at Gösgen is relatively high and could be attributed to partial desaturation of the samples. Such desaturation could have a natural origin (two fluid phases in the formation) or be due to artefacts (evaporation prior to sample sealing, imperfections of the plastic seals, gas exsolution from pore water due to pressure release). It is not currently possible to provide a clear explanation on the basis of only 2 samples. Similar observations were also made for rocks from the Oftringen borehole (Koroleva & Mazurek 2008).

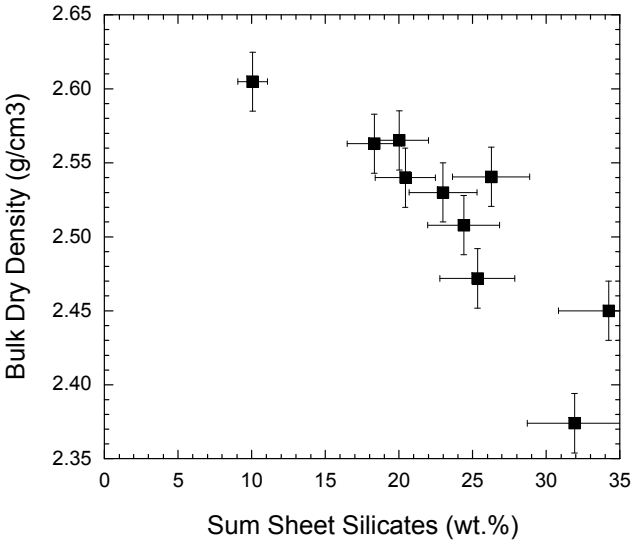

Fig. 5-1: Bulk dry density as a function of of the sum of sheet silicates, which essentially corresponds to the clay content of the Effingen Member.

Error bars indicate the cumulative error (± 10 %) of the XRD measurements and the analytical uncertainty of density measurement (± 0.02 g/cm^3).

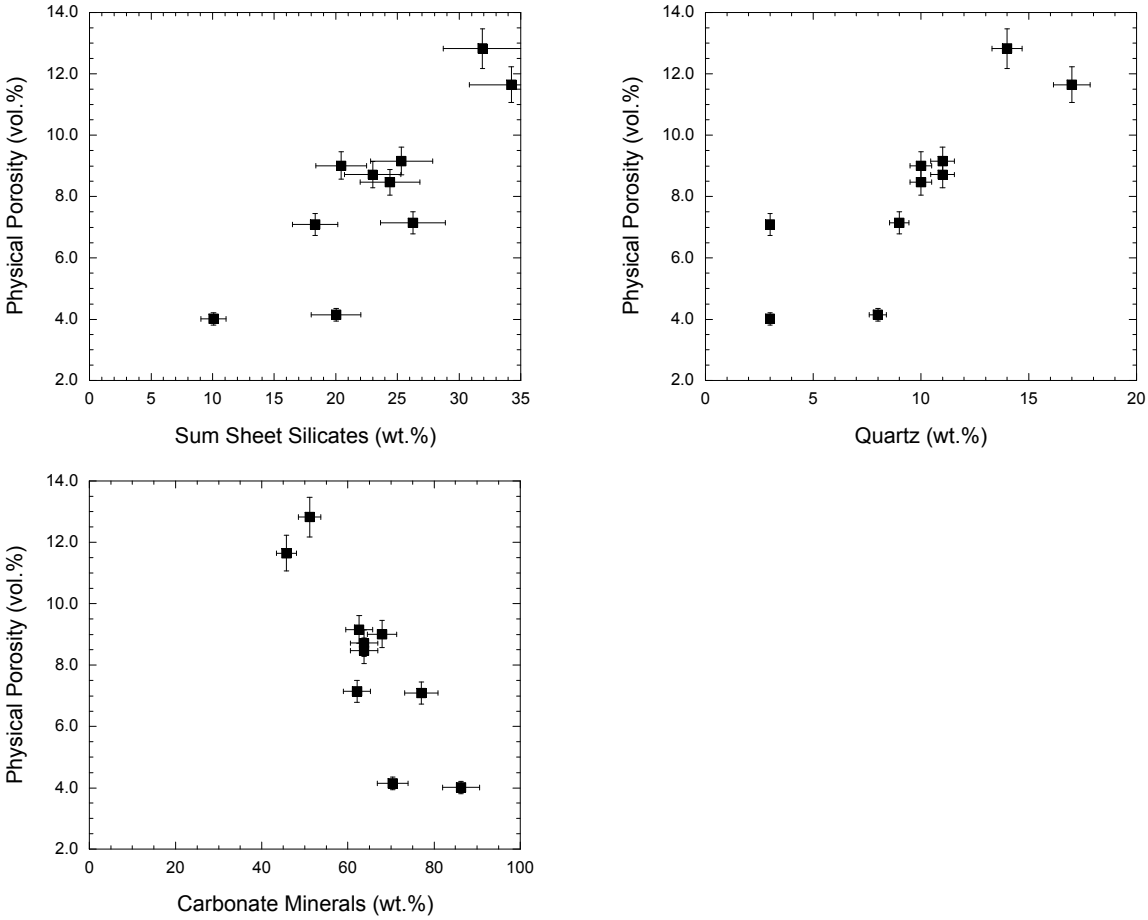

Fig. 5-2: Physical porosity versus the sum of sheet silicates (upper left), quartz (upper right) and total carbonate minerals (lower left) of the Effingen Member.

Error bars indicate a cumulative analytical error of ± 5 % for the physical porosity, ± 10 % for the sum of sheet silicates and ± 5 % for quartz and carbonate mineral contents.

5.3 Specific surface area (BET)

The external specific surface area was determined by nitrogen adsorption isotherms at 150 °C on material of a grain size of ≤ 2 µm of the rock samples from the Effingen Member (Tab. 5-1). It ranges from 6 to 28 m^2/g and and overlaps with the range obtained for the Effingen Member in Oftringen (Koroleva & Mazurek 2008). As expected, the specific surface area correlates positively with the clay content (Fig. 5-3). This is because the clay fraction (< 2 µm) typically has specific surface areas on the order of 15 – 260 m^2/g, depending on the specific clay mineral. On the other hand, silt- and sand-sized minerals (such as calcite and quartz) have specific surface areas of < 10 m^2/g (Feller et al. 1992).

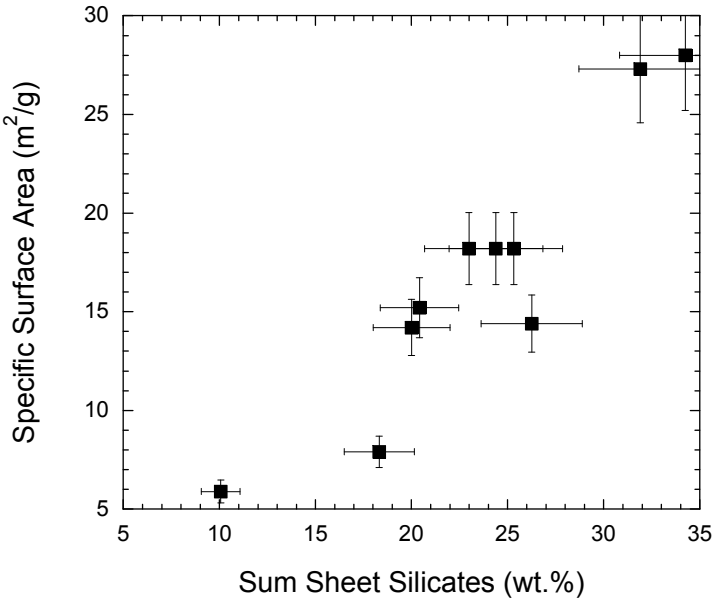

Fig. 5-3: Sum of sheet silicates (i.e. clay content) versus the BET specific surface area of the Effingen Member rocks of the Gösgen borehole KB5a.

Error bars indicate an analytical error of ± 10 % for the sum of sheet silicates and for the BET analysis.

5.4 Water activity

The water activity is defined as the ratio of the vapor pressure of water of a rock sample (p) to the vapor pressure of pure water (p_0) at the same temperature:

$$a_W = \frac{p}{p_o} \tag{9}$$

Measured water activities of the on-site conditioned samples GOS-8 and GOS-9 are 0.85 and 0.87, respectively. These are below that of seawater (0.98) but similar to those observed for the rock samples of the Effingen Member from Oftringen (Koroleva & Mazurek 2008).

In principle, the water activity of a rock sample can be decreased by a) the presence of high salt concentrations in the pore water, b) by clay-water interactions that reduce the proportion of "free" water in the rock samples and c) unsaturated conditions in the pore space. The water activity value in the range 0.85 – 0.87 corresponds to that of a ~ 4 M NaCl solution. As will be shown below, the Cl concentration obtained from the advective displacement experiment is far below that of seawater (Chapter 8). This is evidence that the pore-water salinity alone cannot account for the measured reduced water activity. Furthermore, swelling clay minerals such as smectite and smectite-rich mixed layers are present in only small amounts, meaning that clay-pore water interactions cannot explain the low measured water activity.

Similar to what Koroleva & Mazurek (2008) discussed for the Oftringen borehole, unsaturated conditions, e.g. the presence of a free gas phase in situ, could provide an explanation. However, neither at Oftringen nor at Gösgen there is independent evidence from hydro-tests and/or other investigations for such a free gas phase. Therefore, this hypothesis, based on water activity

measurements on two rock samples alone, has to be treated with caution unless supported by independent data. Possible artefacts such as desaturation of the samples after core recovery, as well as gas exsolution from pore water due to pressure release, also have to be kept in focus.

5.5 Proportion of free water

Accepting that neither the pore water salinity nor the contents of swelling clay minerals significantly contribute to the lowered water activity, an estimate for the ratio of free to bound pore water cannot be readily obtained from the nitrogen adsorption isotherms and the measured water activity values of the rock samples as attempted previously (Koroleva & Mazurek 2008). For samples GOS-8 and GOS-9, such estimates would yield proportions of bound water of 83 % and 77 %, or proportions of free water of 0.17 and 0.23, respectively (Tab. 5-1). These values are similar to the estimates obtained by the same technique for the Effingen Member from Oftringen (Koroleva & Mazurek 2008).

Water activity and degree of saturation are not independent and are affected by the same perturbation of an originally saturated sample. Furthermore, the low values obtained for the water activity are not currently supported by independent measurements and a greatly different ratio is obtained for sample GOS-8 from the comparison of aqueous extraction and advective displacement data (*cf.* Chapter 8). It is therefore concluded that the calculated proportions of free water via water activity need to be considered with great caution.

Tab. 5-1: Petrophysical parameters of rock samples from the Gösgen borehole KB5a.

The original water content has only been preserved in samples GOS-8 and GOS-9 by vacuum packing on-site.

Sample ID	Depth along borehole	Formation	Sum of sheet silicates	Specific surface area	Water Content WC_{wet}	Water Content WC_{dry}	Water-loss porosity	Grain density (average, n = 2)	Bulk wet density, measured (average, n = 4)	Bulk dry density, calc. from bulk wet density (average, n = 4)	Bulk dry density, measured (average, n = 2)	Physical porosity, calc. from calc. bulk dry density	Physical porosity, calc. from measured bulk dry density	Water activity of rock, measured
Unit	[m]		[wt.-%]	[m^2/g]	[wt.-%]	[wt.-%]	[vol.-%]	[g/cm^3]	[g/cm^3]	[g/cm^3]	[g/cm^3]	[vol.-%]	[vol.-%]	-
GOS-1	50.12	OM	7					2.72			2.57		5.8	
GOS-2	63.92	GM	8					2.76			2.62		4.9	
GOS-3	72.77	EM	18	8				2.76			2.56		7.1	
GOS-4	83.21	EM	25	18				2.72			2.47		9.2	
GOS-5	92.85	EM	26	14				2.73			2.54		6.9	
GOS-6	103.04	EM	32	27				2.72			2.37		12.6	
GOS-7	117.38	EM	20	14				2.67			2.57		4.0	
GOS-8	122.89	EM	20	15	2.33	2.39	6.26	2.80	2.60	2.54	2.56	9.0	8.5	0.85
GOS-9	123.71	EM	23	18	2.53	2.60	6.71	2.77	2.59	2.53	2.53	8.8	8.6	0.87
GOS-10	133.08	EM	24	18				2.74			2.51		8.6	
GOS-11	145.59	EM	10	6				2.71			2.60		3.8	
GOS-12	153.31	EM	34	28				2.78			2.45		11.7	

OM: Olten Member, GM: Geissberg Member, EM: Effingen Member

6 Cation Exchange Properties

Cation exchange properties were derived for the two samples GOS-8 and GOS-9 that were preserved in their saturated and reduced state by on-site vacuum-packing. The cation exchange properties were assessed using the Nickel-ethylenediamine (Ni-en) method following the experimental protocol elaborated by Baeyens & Bradbury (1994) and Bradbury & Baeyens (1997/98) as for the samples of the EWS-borehole Oftringen (see Waber 2008b, for details). Ni-en extractions were performed at four different solid:liquid ratios extractions and analyses were made in duplicate.

6.1 Cation exchange capacity

Commonly either the Ni-consumption or the sum of cations analysed in the Ni-en extract solutions is taken as a proxi for the total cation exchange capacity, CEC, depending on the mineralogy of the rock, the composition and the ionic strength of the pore water (Baeyens & Bradbury 1994, Bradbury & Baeyens 1997/98, Waber et al. 2003). As discussed by Waber (2008b), the pore water in the rocks of the Effingen Member of the EWS-borehole Oftringen differ from those known today from the Opalinus Clay at Benken and Mont Terri and from those of the Palfris Marl at Wellenberg. As will be shown in the following chapters, the pore water in the rocks of the Effingen Member of the Gösgen borehole KB5a resembles that in the same rocks at Oftringen and the same limitations apply regarding the derivation of the cation exchange capacity.

Chemical data of the Ni-en extract solutions of the two samples from the Effingen Member at Gösgen are given in Tab. 6-1. For both samples, the Ni-consumption shows a linear correlation with the sum of cations and the values compare well with samples with similar from the Oftringen borehole (Fig. 6-1). The Ni-consumption (about 45 – 56 meq/kg_{rock}) is lower than the sum of cations (about 53 – 66 meq/kg_{rock}). Both samples have similar clay contents (20 – 23 wt.-%) and plot in Fig. 6-1 on the same regression line as given by the samples from the Oftringen borehole. The two Gösgen samples are thus consistent with the explanation given for the Oftringen samples that the greater increase in the sum of cations is attributed to a larger contribution of cations from the pore water compared to induced mineral dissolution during the extraction (*cf.* Waber 2008b), but deliver no further argument because of their almost equal clay content.

For the Gösgen samples a similar behaviour to Oftringen samples with the same total clay content is also observed for the Ni-consumption and sum of cations as a function of solid:liquid ratio (Fig. 6-2). As for the Oftringen samples, some deviations from the established linear relationship is observed at the greatest dilutions, i.e. at solid:liquid ratios of 0.1 and 0.25, as a result of changes in the Ca^{2+} and Mg^{2+} concentrations in the extract solutions (Tab. 6-1). As pointed out by Waber (2008b) a possible, but not yet confirmed explanation for these deviations in the Ni-consumption at lower solid:liquid ratios might be related to some kind of solubility control of Ni by the carbonate system.

The Gösgen samples also follow the same trends given by those from the Effingen Member at Oftringen with respect to the correlation between Ni-consumption with the specific surface area (Fig. 6-3, top left) and between the Ni-consumption and the total clay content (Fig. 6-3, top right). In contrast, illite appears to be a less efficient exchanger at Gösgen (Fig. 6-3, bottom left), but this is almost overcome by the mixed layer minerals (Fig. 6-3, bottom right).

To summarise, the preferable proxi for the CEC in the Effingen Member rocks from the Gösgen borehole KB5a is the Ni-consumption in the Ni-en extract solutions. So derived CEC values agree well with rocks of similar clay contents from the Effingen Member at Oftringen. As in the rocks from Oftringen, the chemical type of the aqueous extract solutions (Na-SO_4-Cl, see Chapter 7) inhibits an accurate correction of the sum of cations measured in the Ni-en extract solutions.

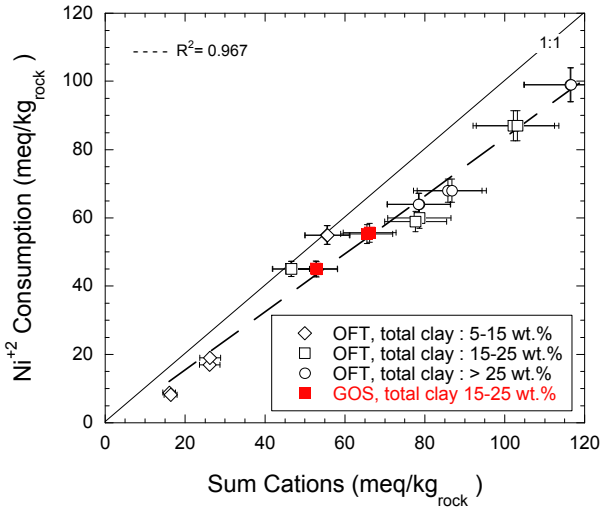

Fig. 6-1: Relationship between the sum of cations and the Ni-consumption measured in the Ni-en extract solutions and as a function of the clay content of drillcore samples from the Effingen Member.

Samples labelled "GOS" are from the Gösgen borehole KB5a, those labelled "OFT" from the EWS-borehole Oftringen are given for comparison.

Error bars indicate analytical error of ± 5 % for Ni and ± 10 % for the sum of cations in the Ni-en extract solutions.

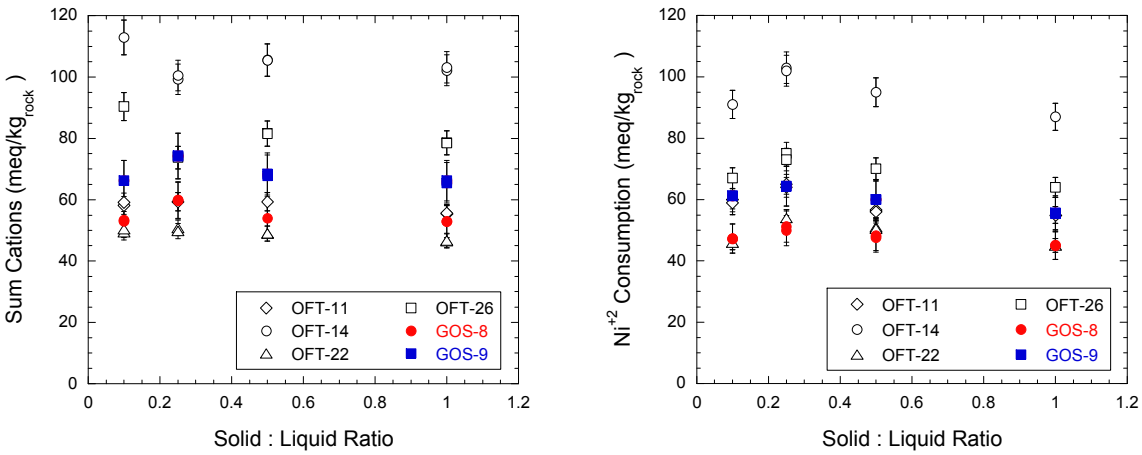

Fig. 6-2: Relationship between the sum of cations (left) and the Ni-consumption (right) measured in the Ni-en extract solutions and the solid:liquid ratio used in the extractions.

Samples labelled "GOS" are from the Gösgen borehole KB5a, those labelled "OFT" from the EWS-borehole Oftringen are given for comparison.

Error bars indicate analytical error of ± 10 % for the sum of cations and ± 5 % for Ni in the Ni-en extract solutions.

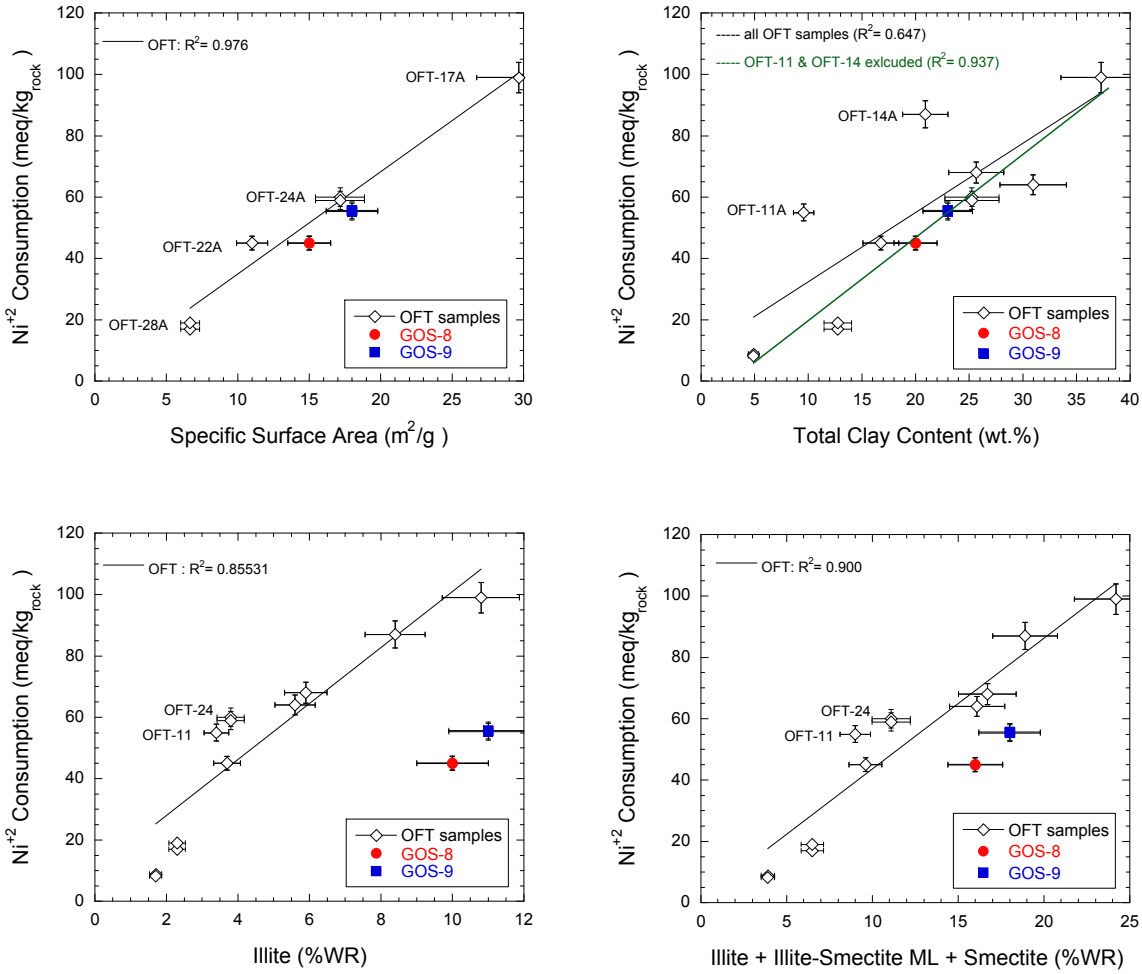

Fig. 6-3: Relationship between the Ni-consumption in the Ni-en extract solutions as proxy for the CEC of the rocks and the specific surface area (top left), the total clay content (top right), the illite content (bottom left) and the sum of illite- and smectite-type minerals (bottom right).

Samples labelled "GOS" are from the Gösgen borehole KB5a, those labelled "OFT" from the EWS-borehole Oftringen are given for comparison.

Error bars indicate analytical error of ± 5 % for Ni and ± 10 % for the specific surface area and the clay contents of the rocks.

Tab. 6-1: Chemical analyses of Ni-en extract solutions

a, b represent duplicate extractions.

Sample	Units	GOS-8A		GOS-8B		GOS-8C		GOS-8D	
		a	b	a	b	a	b	a	b
Borehole Length	[m]	122.89		122.89		122.89		122.89	
Rock Type		sandy argillaceous limestone						sandy argill. limestone	
Solid – Liquid Ratio		1.0	1.0	0.5	0.5	0.25	0.25	0.1	0.1
pH (lab)	[-log(H^+)]	8.93	8.93	8.42	8.41	8.32	8.33	8.14	8.14
Sodium (Na^+)	[meq/kg_{rock}]	20.8	20.7	20.5	20.5	20.7	20.3	20.4	20.4
Potassium (K^+)	[meq/kg_{rock}]	6.9	7.2	7.5	7.4	8.1	8.1	8.2	8.1
Magnesium (Mg^{2+})	[meq/kg_{rock}]	9.6	9.6	9.7	9.7	11.2	11.3	9.5	9.4
Calcium (Ca^{2+})	[meq/kg_{rock}]	15	14.9	15.8	15.9	19.3	19.4	14.8	14.5
Strontium (Sr^{2+})	[meq/kg_{rock}]	0.52	0.52	0.51	0.51	0.55	0.56	0.52	0.52
Sum Cations	[meq/kg_{rock}]	52.8	52.9	54.0	54.0	59.9	59.7	53.4	52.9
Ni-Consumption	[meq/kg_{rock}]	45.1	44.9	48.2	47.6	49.9	51.2	47.2	47.3

Sample	Units	GOS-9A		GOS-9B		GOS-9C		GOS-9D	
		a	b	a	b	a	b	a	b
Borehole Length	[m]	123.71		123.71		123.71		123.71	
Rock Type		sandy argillaceous limestone							
Solid – Liquid Ratio		1.0	1.0	0.5	0.5	0.25	0.25	0.1	0.1
pH (lab)	[-log(H^+)]	8.85	8.86	8.39	8.39	8.3	8.3	8.14	8.14
Sodium (Na+)	[meq/kg_{rock}]	25.5	25.9	25.7	25.8	25.7	26	25.5	25.5
Potassium (K^+)	[meq/kg_{rock}]	9.6	9.8	10	10.1	11.3	11.1	11.3	11.3
Magnesium (Mg^{2+})	[meq/kg_{rock}]	11.7	11.7	12	12.2	13.5	13.6	11.2	11.2
Calcium (Ca^{2+})	[meq/kg_{rock}]	18.1	18.2	19.5	19.7	23	22.9	17.6	17.6
Strontium (Sr^{2+})	[meq/kg_{rock}]	0.63	0.63	0.63	0.63	0.67	0.68	0.62	0.62
Sum Cations	[meq/kg_{rock}]	65.5	66.2	67.8	68.4	74.2	74.3	66.2	66.2
Ni-Consumption	[meq/kg_{rock}]	55.3	55.7	60.0	60.1	64.3	64.4	61.3	61.2

6.2 Cation-exchange population and selectivity coefficients

Cation concentrations in the Ni-en extract solutions are similar for samples GOS-8 and GOS-9 and show the same trends as a function of solid:liquid ratio (Fig. 6-4). Highest concentrations are observed for Na^+ and Ca^{2+}, followed by Mg^{2+} and K^+ and small amounts of Sr^{2+} (Tab. 6-1). For Na^+ and Sr^{2+} equal concentrations are observed for all different solid:liquid ratios, whereas some variation occurs in the concentrations of Ca^{2+}, Mg^{2+} and K^+ (Fig. 6-4). In all these characteristics, the Gösgen samples thus compare well with Effingen Member samples of similar clay content from the EWS-borehole Oftringen (*cf.* Waber 2008b).

The derivation of the *in situ* cation-exchange population and the cation-exchange selectivity coefficients require a well-supported correction of the measured cation inventories in the Ni-en extract solutions for contributions from the pore water and from mineral dissolution during the extraction. As discussed in Waber (2008b), in this derivation the ratios of Na/Ca, Ca/SO_4 and SO_4/Cl in the Ni-en extract and aqueous extract solution are of special importance because it was basically developed for Na-Cl dominated pore water and cation exchange systems such as the Palfris-Formation and the Opalinus Clay (Baeyens & Bradbury 1994, Bradbury & Baeyens 1997/98). Samples GOS-8 and GOS-9, both treated with on-site presservation and all extractions performed under controlled oxygen-free conditions, show the same relationship between Na^+ and Ca^{2+} in the Ni-en extract solutions (Fig. 6-5) and have similar Ca/SO_4 and SO_4/Cl ratios in the aqueous extract solutions (*cf.* Chapter 7). Because of this similarity in the Ni-en extract and aqueous extract solution compositions of samples from the Effingen Member from Gösgen and Oftringen, the same restrictions and reservations as made for the Oftringen rocks apply for the derivation of the *in situ* exchangable cation population, fractional occupancies and cation-exchange selectivity coefficients for the Gösgen rocks.

Bearing all these reservations in mind, similar values are calculated for the two samples from the Gösgen borehole KB5a for exchangeable cation population, the fractional occupancies and the cation-exchange selectivity coefficients (Tab. 6-2) as for the Effingen Member rocks from the EWS-borehole Oftringen (*cf.* Waber 2008a). As for these, the calculated exchangeable population and fractional occupancy are in similar contradiction to other, more reliable observations made about the pore water in the rocks of the Effingen Member such as the advective displacement experiment. The calculated selectivity coefficients (based on the Gaines-Thomas convention), which, in some cases, deviate strongly from values known from the literature further support the unreliability of the applied correction model.

To conclude, the cation-exchange capacity of the rocks from the Effingen Member is well described by the Ni-consumption in the Ni-en extract solutions. The CEC of the two argillaceous limestone samples from the Gösgen borehole KB5a varies between 45 and 56 meq/kg_{rock}. The same conclusions as for the Effingen Member rocks at Oftringen apply for the *in situ* exchangeable populations and selectivity coefficients. These values cannot be obtained from the produced data due to a yet unknown perturbation either by not further identified mineral dissolution during the extraction or a not further quantifiable contribution of reactive components, especially Ca^{2+} and SO_4^{2-} from the pore water. In order to derive reliable selectivity coefficients, adsorption isotherms need to be derived for each cation over the range of clay contents and composition of the rocks of the Effingen Member.

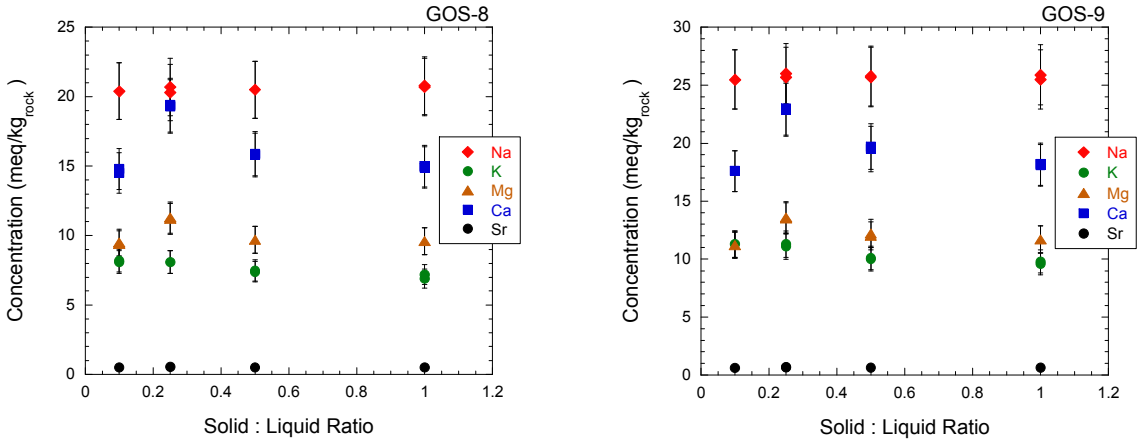

Fig. 6-4: Major cation concentrations in Ni-en extract solutions as a function of the solid:liquid ratio used in the extraction.

Error bars indicate analytical error of ± 10 %.

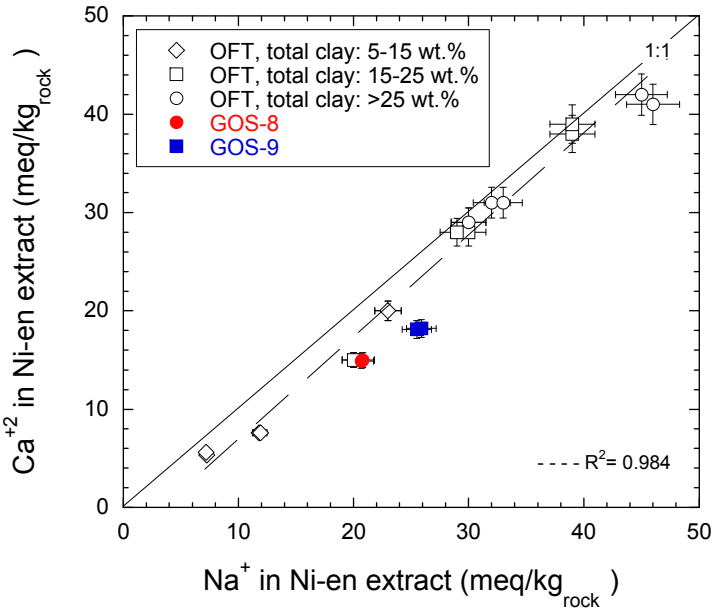

Fig. 6-5: Inventory of Na^+ versus that of Ca^{2+} in Ni-en extract solutions as a function of the total clay content of the rocks from the Effingen Member from Gösgen (GOS-8 and GOS-9) and Oftringen (OFT).

The total clay content of samples GOS-8 and GOS-9 is 20 wt.-% and 23 wt.-%, respectively. Error bars indicate analytical error of ± 5 %.

Tab. 6-2: Calculated exchange population, fractional occupancy and selectivity coeffi-cients. The values are not representative for *in situ* conditions.

Sample	**GOS-8**	**GOS-8**	**GOS-9**	**GOS-9**
	Average	**Average**	**Average**	**Average**
Borehole Length	122.89	122.89	123.71	123.71
Rock Type	sandy-argill. limestone	sandy-argill. limestone	sandy-argill. limestone	sandy-argill. limestone
Solid – Liquid Ratio	1.00	1.00	1.00	1.00
Corrected Exchange Population	Case I	Case II	Case I	Case II
	Cl	Cl + SO_4	Cl	Cl + SO_4
K [meq/kg_{rock}]	7.10	7.10	9.70	9.70
Na [meq/kg_{rock}]	16.99	12.38	20.39	15.46
Ca [meq/kg_{rock}]	15.00	15.00	18.20	18.20
Mg [meq/kg_{rock}]	9.60	9.60	11.70	11.70
Sr [meq/kg_{rock}]	0.52	0.52	0.63	0.63
Sum Cations [meq/kg_{rock}]	49.2	44.6	60.62	55.69
Ni Consumption [meq/kg_{rock}]	45.0	45.0	55.5	55.5
Fractional Occupancy				
NK	0.144	0.159	0.160	0.174
NNa	0.345	0.278	0.336	0.278
NCa	0.311	0.343	0.307	0.334
NMg	0.199	0.220	0.197	0.215
NSr	0.011	0.012	0.010	0.011
Selectivity Coefficients				
log K-Na	0.685	0.822	0.742	0.862
log Ca-Na	0.343	0.575	0.435	0.639
log Mg-Na	-0.041	0.097	0.029	0.150
log Sr-Na	0.256	0.489	0.487	0.691

7 Aqueous Extraction

Aqueous extraction tests on material from the Gösgen borehole KB5a were performed on each 1 sample from the Olten and Geissberg Members and 10 samples from the upper part of the Effingen Member. Material from the central part of the drillcore was used for al samples to exclude any contamination from the drilling process. Except for two samples all handling was conducted under ambient conditions. Extract solutions were prepared in duplicate and for these latter samples only analysed for their anion concentrations (Tab. 7-1). Samples GOS-8 and GOS-9 were prepared and extracted at different solid:liquid ratios in an oxygen-free atmosphere in a glovebox to minimise oxidation of the rock. For these two samples a complete chemical analysis was performed. As shown in Tab. 7-2, the quality of these 16 analyses is excellent with respect to charge balance (better than ± 4 % for all samples, average 1.43 % ± 1.22 %) and the agreement between duplicate extractions.

7.1 Identification of chemically conservative and reactive components

Performing extractions at different solid:liquid ratios yields certain information about the chemical behaviour of an element during aqueous extraction. Combined with information about the mineralogical composition of the rocks and the mineral saturation states in the extract solutions, the sinks and sources of the various elements can be identified. Within this context it needs to be mentioned, however, that a linear behaviour of an element concentration as a function of soid:liquid ratio does not necessarily prove a conservative behaviour because for a certain element such a relationship would also be produced by kinetically reacting solid phases that are completely or incompletely dissolved at each solid:liquid ratio, although not reaching a solubility control by a secondary precipitate.

Aqueous extractions at four different solid:liquid ratios were performed on the two argillaceous limestone samples samples GOS-8 (122.89 m borehole length) and GOS-9 (123.71 m borehole length) from the Effingen Member (Tab. 7-2). For both samples, Cl^- and SO_4^{2-} show an excellent linear correlation with increasing solid:liquid ratio of the extraction test and that passes – within the analytical error – through the origin (Fig. 7-1). The concentration of SO_4^{2-} is higher than that of Cl^- at all solid:liquid ratios. A solid source for these components appears to be absent because a) no solid Cl-salts and sulphate minerals were observed by X-ray diffractometry (*cf.* Chapter 4), b) all extract solutions of all solid:liquid ratios are under-saturated with respect to gypsum by at least two orders of magnitude (Tab. 7-3), c) Sr^{2+} concentrations in all extract solutions below a detection limit of 1 mg/L (Tab. 7-2), which inhibit a measurable contribution from celestite dissolution, and d) the linear correlation obtained for SO_4^{2-} that indicates no significant sulphide mineral dissolution (i.e. pyrite oxidetion) what would result in a non-linear relationship. This suggests that Cl^- and SO_4^{2-} behave conservatively during the conducted aqueous extractions under oxygen-free conditions. For samples GOS-8 and GOS-9 the pore water of rocks from the Effingen Member is thus the only Cl^- and SO_4^{2-} source as it was already observed for the samples from the EWS-borehole Oftringen (*cf.* Waber 2008c).

In contrast to Cl^- and SO_4^{2-}, F^- and total alkalinity behave differently during aqueous extraction (Fig. 7-1). The components show a non-linear correlation with increasing solid:liquid ratios and their concentrations are influenced by mineral dissolution and possibly other reactions. In addition, the analytical uncertainty for F^- is somewhat larger (about 10 %) than for the other elements due to a not further resolvable overlap with low-molecular weight organic acids during ion-chromatographic elution. A similar behaviour was also observed for these two compounds in the extract solutions of Effingen Member rocks from the EWS-borehole Oftringen, and the same processes as described for these rocks might also apply for those of the Gösgen borehole

KB5a (*cf.* Waber 2008c). Within this context it should be noted that all extract solutions are under-saturated with respect to the major sources for F^- and total alkalinity, which are fluorite and dolomite (Tab. 7-3).

For Br^-, the chemical behaviour (i.e. conservative versus reactive) during extraction cannot be evaluated because the concentrations are below the detection limit of 0.5 mg/L in the majority of the extract solutions (Tab. 7-2). No quantification was performed for I^- in these samples.

For the major cations, the concentration behaviour as a function of solid:liquid ratios indicate that they all are involved in some type of reactions. The concentrations of Na^+ and K^+ show a well-defined linear relationship (Fig. 7-2), what is in contrast to the samples from the EWS-borehole Oftringen (Waber 2008c). The intercept of the regression line is, however, above the origin indicting a contribution from a kinetically quick reaction. As for the rocks from EWS-borehole Oftringen this indicates that both these elements are also involved in cation exchange reactions.

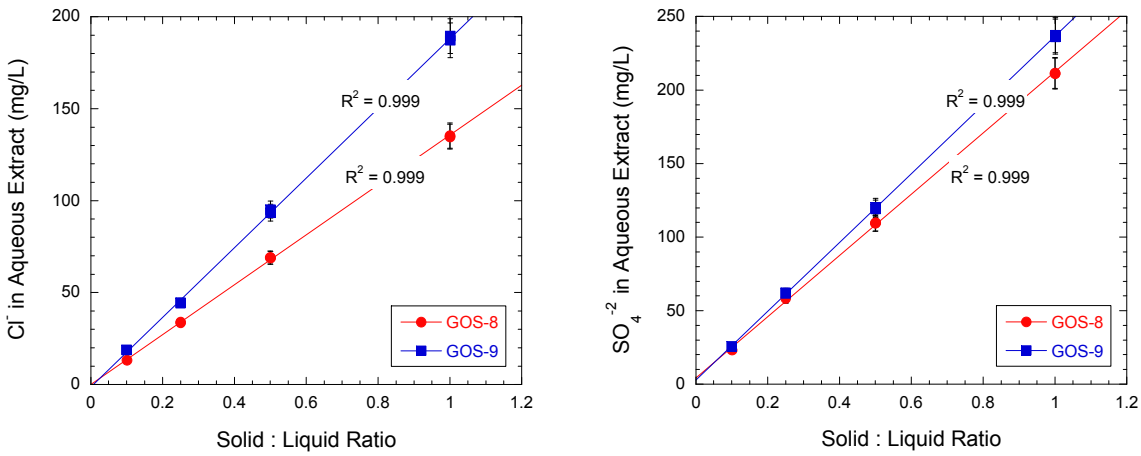

Fig. 7-1: Concentrations of Cl^-, SO_4^{2-}, F^- and total alkalinity in aqueous extract solutions of the glovebox-prepared samples GOS-8 and GOS-9 at different solid:liquid ratios.

R is the correlation coefficient of the linear fit; error bars indicate an analytical error of ± 5 % and ± 10 % for fluoride (see text).

In contrast to Na^+ and K^+, the concentrations of Ca^{2+} and Mg^{2+} are low in the extract solution at all solid:liquid ratios of the four samples (Fig. 7-2). For both compounds, the concentrations show a curved behaviour as a function of increasing solid:liquid ratio indicating the involvement in chemical reactions during extraction. Such reactions include the dissolution of calcite and dolomite. The low concentrations further indicate that Ca^{2+} and Mg^{2+} get also removed again from the extract solutions by exchanging with Na^+ and K^+ from the clay surface sites due to the induced reduction of the *in situ* persisting ionic strength during aqueous extraction. Thus, the concentrations of Ca^{2+} and Mg^{2+} in the aqueous extract solution are the product of multiple sources and sinks.

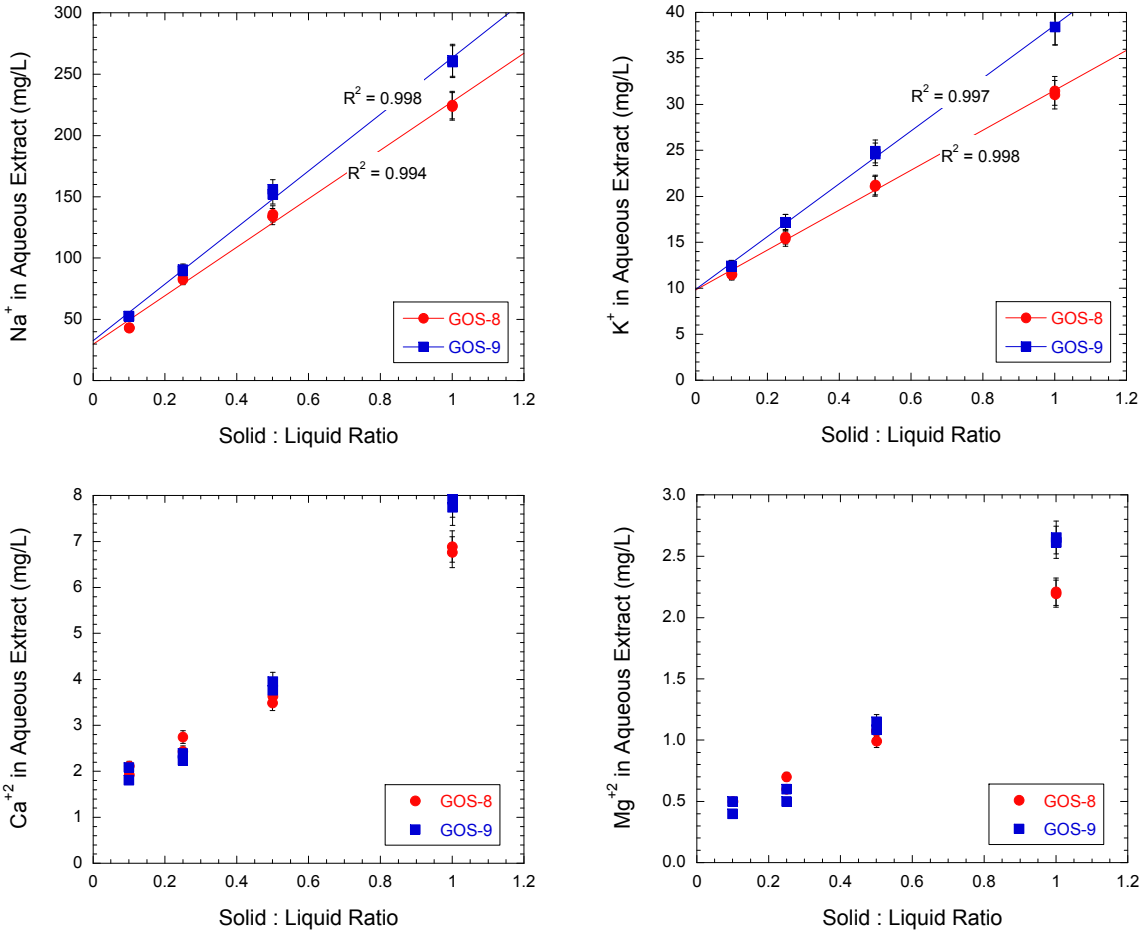

Fig. 7-2: Concentrations of Na^+, K^+, Ca^{2+} and Mg^{2+} in aqueous extract solutions of the glovebox-prepared samples GOS-8 and GOS-9 at different solid:liquid ratios.

R is the correlation coefficient of the linear fit; error bars indicate an analytical error of ± 5 %.

7.2 Chemical composition and mineral saturation states

At a solid:liquid ratio of 1, the total mineralisation of aqueous extract solutions of samples GOS-8 and GOS-9 are about 780 mg/L and 915 mg/L and are within the range given by the Effingen Member samples from the EWS-borehole Oftringen (590 – 1100 mg/L). The chemical type of the extract solutions changes from of a Na-HCO_3-SO_4-Cl type at lowest solid:liquid ratio to a Na-SO_4-Cl-HCO_3 and Na-Cl-SO_4-Cl-HCO_3 type at highest solid:liquid ratio (Fig. 7-3). As shown above, the sulphate in the extract solution appears to originate only from the pore water, whereas the bicarbonate also stems from carbonate mineral dissolution, which is most pronounced at lowest solid:liquid ratio.

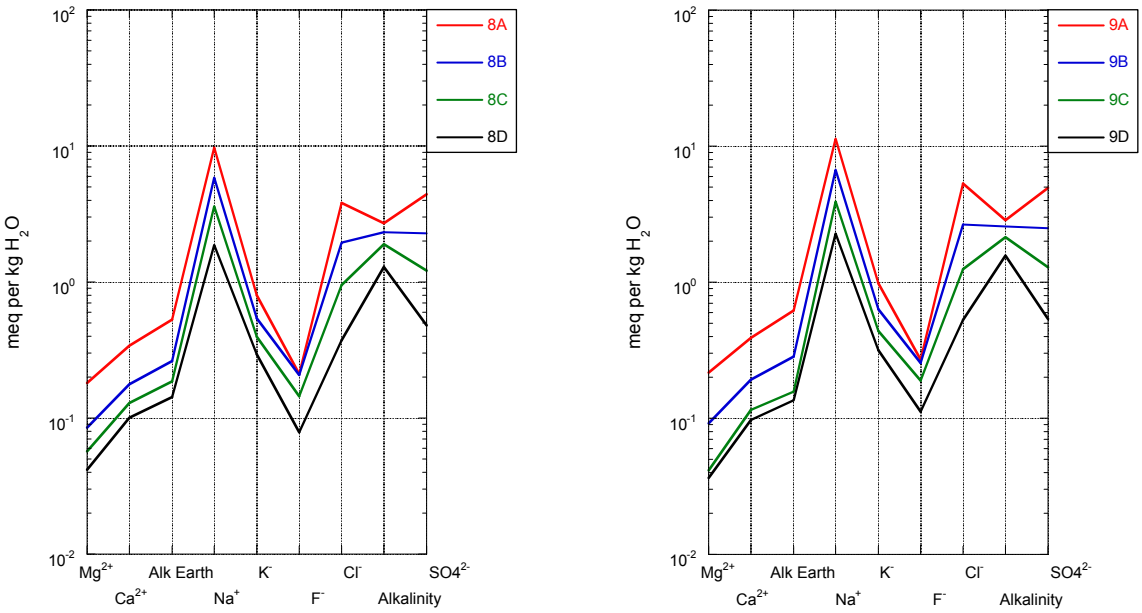

Fig. 7-3: Schoeller diagram of the aqueous extract solution at different solid:liquid ratios (A = 1.0, B = 0.5, C = 0.25, D = 0.1) of samples GOS-8 and GOS-9 from the Effingen Member of the Gösgen borehole KB5a.

Clearly visible is the change from a Na-HCO_3 chemical type to a Na-SO_4-Cl chemical type as a function of increasing solid:liquid ratio. Note that HCO_3 stems mainly from mineral dissolution reactions during the extraction (see text).

7.2.1 Chloride and bromide

In section 7.1 it was shown that during aqueous extraction the Cl^- concentrations behave chemically conservatively. A similar behaviour can be assumed for the Br^- concentrations although this cannot be confirmed by the present data, because of Br^- concentrations below the detection limit of the applied analytical technique in extraction test with solid:liquid ratios of less than 1. By accepting this assumption, however, the Br/Cl ratio might be used to discriminate between fresh water and seawater origin of the pore water extracted from the rocks.

At a solid:liquid ratio of 1, the concentrations of Cl^- in the extract solutions of rocks from the Effingen Member vary between about 48 mg/L and 340 mg/L (Tabs. 7-1 and 7-2) and are similar to the those from the EWS-Borehole Oftringen (64 – 308 mg/L). If measurable at all, the Br^- concentrations are all between 0.5 – 1.2 mg/L just above the detection limit of the applied method. In contrast to the extract solution from the Effingen Member at Oftringen, however, the Br/Cl ratios of the extract solutions from the Gösgen samples plot closer to the seawater dilution line (Fig. 7-4). However, the Br/Cl ratios should be regarded with caution and the Br^- concentrations need to be confirmed by an independent analytical method with a higher precision at low Br^- concentrations than the applied ion-chromatographic technique as already mentioned for the Oftringen samples (*cf.* Waber 2008c).

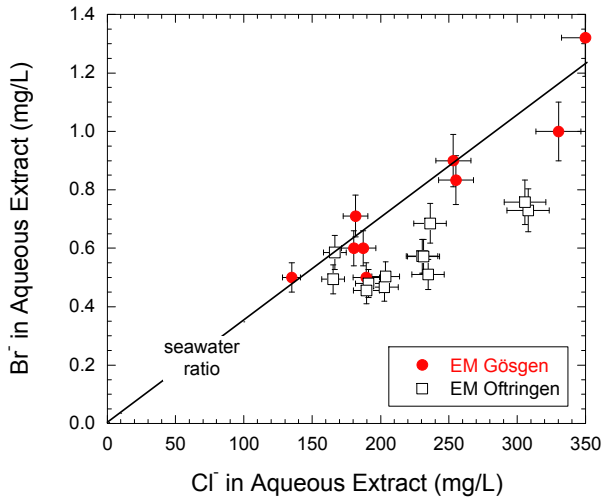

Fig. 7-4: Concentrations of Br^- versus Cl^- in the aqueous extract solution a solid:liquid ratio of 1 of rocks from the Effingen Member of the Gösgen borehole (EM Gösgen) and the EWS-borehole Oftringen (EM Oftringen) and compared to the Br/Cl seawater ratio.

Error bars indicate analytical error of ± 5 % for Cl and ± 10 % for Br.

7.2.2 Sulphate

As for the rocks from the Effingen Member of Oftringen it appears that SO_4^{2-} behaves conservatively during the extraction process and no measurable perturbation by sulphate mineral dissolution and/or pyrite oxidation can be observed if the samples were prepared under oxygen-free conditions (*cf.* Section 7.1). Also in the extract solutions of the Gösgen rocks no trend is established between the SO_4^{2-} concentrations in the extract solutions and the total sulphur contents in the rocks (Fig. 7-5). In the glovebox-prepared samples GOS-8 and GOS9, the SO_4^{2-} concentrations are lower by a factor of about 2 – 2.5 compared to the samples prepared under ambient conditions (*cf.* Tabs. 7-1 and 7-2). This highlights the effect of pyrite oxidation during extraction under ambient conditions. It further supports the association of the total sulphur contents in the rocks to the pyrite present as outlined in Chapter 4.

Extract solutions of the glovebox-prepared samples GOS-8 and GOS-9 have SO_4^{2-} concentrations of about 211 – 237 mg/L similar to those found in the Effingen Member rocks of Oftringen (124 – 325 mg/L). Also at Gösgen the SO_4^{2-} concentrations are higher than those of Cl^- and SO_4^{2-} constitutes the dominant anion in the extract solutions of samples GOS-8 and GOS-9 (Tab. 7-2). The aqueous extract solutions of these two samples are grossly under-saturated with respect to gypsum (SI_{gypsum} = -2.27 to -3.60) and celestite ($SI_{celestite}$ = -1.67 to -1.75; Tab. 7-3), similar as it was also calculated for the extract solutions from the Oftringen rocks (Waber 2008c).

The SO_4/Cl ratio of samples GOS-8 and GOS-9 is higher than that of seawater and seawater can be excluded for at least a large amount of the SO_4^{2-} and/or the Cl^- present in the pore water (Fig. 7-6). The different trends suggested in Fig. 7-6 for the SO_4/Cl ratio of samples prepared in the glovebox and under ambient conditions do not bear any further information about the *in situ* pore water because of SO_4^{2-} derived from pyrite oxidation during extraction under ambient conditions. For these samples the Figure 7-6 thus simply illustrates the difference in SO_4^{2-} concentrations between the different conditions during aqueous extraction.

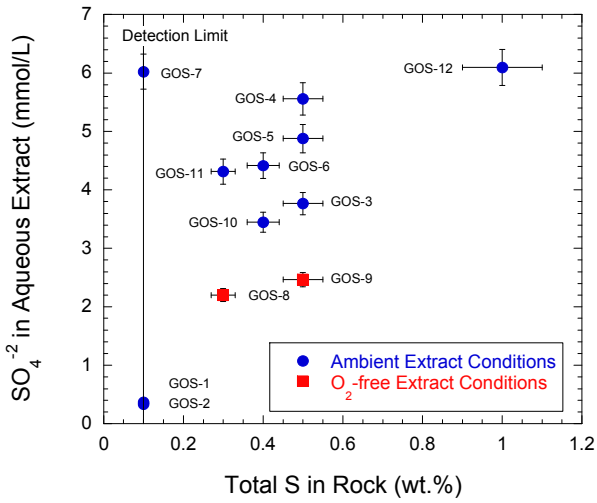

Fig. 7-5: Concentrations of SO_4^{2-} in the aqueous extract solution at solid:liquid ratio of 1 versus the total sulphur content of rocks from of the Gösgen borehole KB5a.

Samples GOS-1 and GOS-2 are limestones from the Olten and Geissberg Members. Error bars indicate analytical error of ± 5 % for ion-chromatographic analyses and ± 10 % for CS-Mat analyses (total S in rock, *cf.* Tab. 4-1).

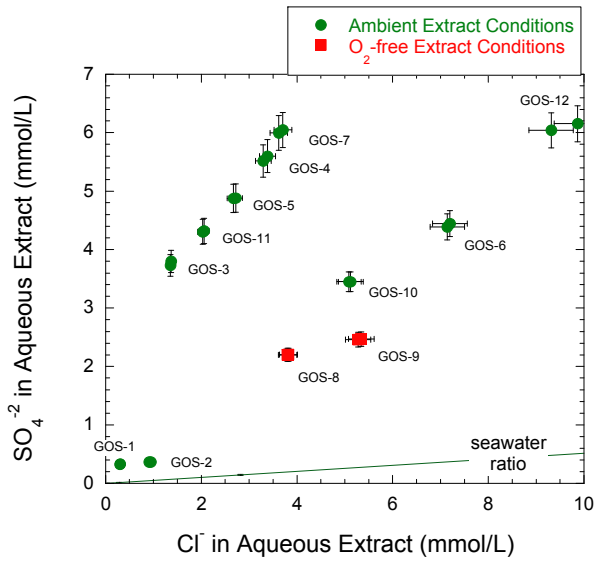

Fig. 7-6: Concentrations SO_4^{2-} versus those of Cl^- in the aqueous extract solution at solid:liquid ratio of 1 of rocks from the rocks of the Gösgen borehole KB5a.

Samples GOS-1 and GOS-2 are limestones from the Olten and Geissberg Members. Error bars indicate analytical error of ± 5 %.

7.2.3 Fluoride

As mentioned in section 7.1, the analytical uncertainty for F^- might be somewhat larger (about 10 %) than for the other elements due to a not further resolvable overlap with low-molecular weight organic acids during ion-chromatographic elution. The analysed concentrations in extract solution of rocks from the Effingen Member vary between 3.7 mg/L and 11.8 mg/L

(Tab. 7-1) and there is no systematic variation of the contents with sample depth. In contrast to the Effingen Member rocks from Oftringen, the extract solutions of samples GOS-8 and GOS-9 are under-saturated with respect to fluorite ($SI_{fluorite}$ = -0.60 to -2.03; Tab. 7-3).

7.2.4 Sodium and potassium

In the extract solutions of samples GOS-8 and GOS-9 Na^+ is the dominant and K^+ the second most abundant cation with concentrations between 224 – 261 mg/L and 31 – 38 mg/L (Tab. 7-2). The Na^+ concentrations are similar to those obtained for extract solution of rocks from the Effingen Member of the EWS-borehole Oftringen (175 – 341 mg/L), whereas those for K^+ are much higher than in the solutions from the Oftringen rocks (9 – 24 mg/L).

As mentioned in section 7.1, the concentrations of Na^+ and in particular that of K^+ in the extract solutions of samples GOS-8 and GOS-9 display a better correlation with the solid:liquid ratio than those in the extract solution of the Effingen Member rocks from EWS-borehole Oftringen. As a function of the total clay faction, the Na^+ concentrations of the Gösgen samples describe the same trend as the Oftringen samples (Fig. 7-7, left). In contrast, the K^+ concentrations of the Gösgen samples deviate strongly from trend given by the Oftringen samples as a function of the sum of illite and mixed layer minerals (Fig. 7-7, right). It appears that this different behaviour is due to the different ratios of illite to illite-smectite mixed layer minerals in the rock. In the clay faction of the two Gösgen samples the ratio illite to illite-smectite mixed layers is 1.8 (all samples: 1.5 ± 0.4, n = 10), whereas it is 0.7 ± 0.2 (n = 19) in the clay fraction of the Oftringen samples (*cf.* Chapter 4). This suggests that the differences in the K^+ concentrations of extract solutions of Effingen Member rocks from the two sites are related to differences in the cation exchange behaviour of the rocks. This highlights the importance of cation exchange reactions as a function of clay composition in the rocks of the Effingen Member.

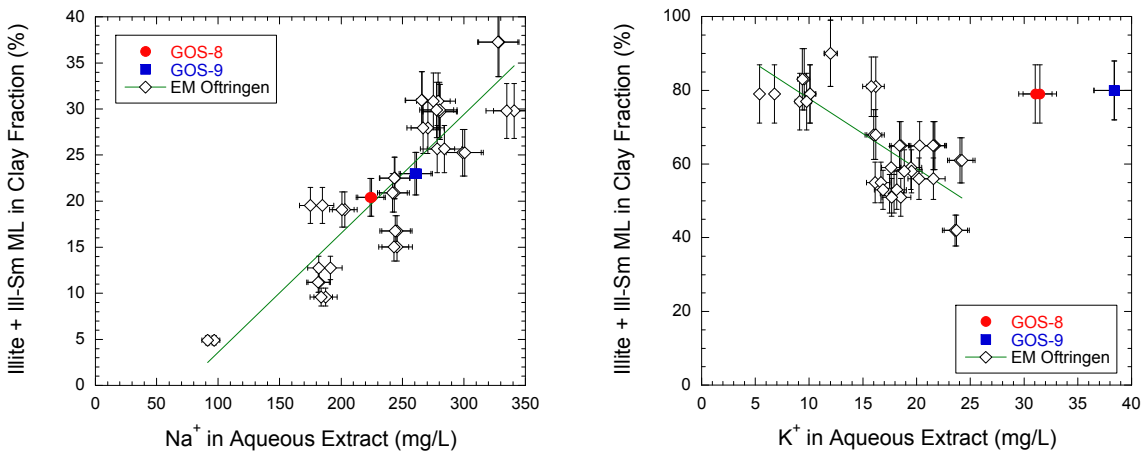

Fig. 7-7: Concentrations of Na^+ and K^+ in the aqueous extract solutions (S:L = 1:1) of samples GOS-8 and GOS-9 versus the total clay content and the sum of illite and illite-smectite mixed layers in the clay fraction, respectively, in comparison to the Effingen Member rocks from the EWS-borehole Oftringen.

Error bars indicate analytical error of ± 5 % for solution concentrations and ± 10 % for the mineralogical data.

7.2.5 Alkalinity, pH and alkaline earth elements

For samples GOS-8 and GOS-9, aqueous extraction was performed in an oxygen-free glovebox under an N_2 stream and so was the pH measurement and alkalinity titration of the filtered supernatant extract solutions. The pH values of these extract solutions range between about 8.7 and 9.5 (Tab. 7-2) and compare well with those from Effingen Member extract solutions from the EWS-borehole Oftringen (pH = 8.7 – 9.3). Using the measured values for pH, total alkalinity and Ca^{2+}, calcite is slightly super-saturated ($SI_{calcite}$ = 0.17 ± 0.08) in the aqueous extract solutions at corresponding partial pressures of CO_2 below atmospheric (log pCO_2 = -4.12 ± 0.35; Tab. 7-3). Similar was observed for the extract solutions from Effingen Member rocks from the EWS-borehole Oftringen ($SI_{calcite}$ = 0.33 ± 0.13, log pCO_2 = -3.96 ± 0.26; Waber 2008c). As mentioned for these rocks such super-saturation and low pCO_2 are geochemically unreasonable and due to the fact that the pH measurement and alkalinity titration were performed in an essentially CO_2-free atmosphere in the glovebox leading to out-gassing of CO_2 from the extract solution during measurement. By adjusting the solutions to calcite equilibrium by adding back the lost CO_2 using geochemical modelling, the corrected pH of the solutions range between 8.5 and 9.4 (Oftringen: 7.8 – 9.2) and with associated pCO_2 values around atmospheric (log pCO_2 = -3.88 ± 0.40; Tab. 7-3; Oftringen; -3.53 ± 0.28). Under these conditions disordered dolomite is still grossly under-saturated ($SI_{dolomite}$ = -0.80 ± 0.04; Oftringen: -0.98 ± 0.10) as would be expected after an extraction time of only 24 hours.

Concentrations of Ca^{2+} and Mg^{2+} are low in the extract solutions of samples GOS-8 and GOS-9 and vary between 1.8 and 7.9 mg/L and 1.0 and 2.7 mg/L, respectively (Tab. 7-2). The concentrations are thus in the same range as those given by the Effingen Member extract solutions from the EWS-borehole Oftringen (Ca^{2+} = 3.4 – 12.3 mg/L and Mg^{2+} = 0.8 – 3.1 mg/L). These concentrations cannot be further interpreted in terms of pore water because they are the product of multiple processes which occur during the extraction such as cation exchange and mineral dissolution/precipitation as also proven by their non-linear behaviour as a function of the solid:liquid ratio of the extraction (*cf.* Section7-1).

Concentrations of Sr^{2+} are only above the detection limit of the applied method in a few samples (Tab. 7-2). For the few samples where Sr data were available an under-saturation with respect to strontianite ($SrCO_3$; $SI_{strontianite}$ = -0.64 ± 0.10) is calculated at calcite equilibrium (Tab. 7-3) similar as for the extract solution from Oftringen samples ($SI_{strontianite}$ = -0.40 ± 0.20).

Tab. 7-1: Anion concentrations of aqueous extract solutions.

a, b represent duplicate extractions.

Aqueous Extract Solution	Unit	GOS-1A		GOS-2A		GOS-3A		GOS-4A	
		a	b	a	b	a	b	a	b
Sample Description									
Borehole Length	[m]	50.12		63.92		72.77		83.21	
Stratigraphy		Olten M.		Geissberg M.		Effingen M.		Effingen M.	
Rock Type		limestone		limestone		argillaceous limestone		sandy-calcareous marl	
Experiment Time	[hours]	24	24	24	24	24	24	24	24
Solid – Liquid Ratio (S:L)		1.000	1.000	1.000	1.000	1.000	1.000	1.000	1.000
Conditions		ambient	ambient	ambient	ambient	ambient	ambient	ambient	ambient
Sample Temperature	[ºC]	20	20	20	20	20	20	20	20
Fluoride (F^-)	[mg/L]	2.5	3.0	2.3	2.4	2.5	2.6	5.5	5.3
Chloride (Cl^-)	[mg/L]	10.6	10.8	33.7	32.3	48.4	48.1	120.0	116.8
Bromide (Br^-)	[mg/L]	< 0.5	< 0.5	< 0.5	< 0.5	< 0.5	< 0.5	< 0.5	< 0.5
Sulphate (SO_4^{2-})	[mg/L]	31.5	31.6	35.1	35.3	365.1	358.6	538.0	529.9
Nitrate (NO_3^-)	[mg/L]	< 1	< 1	< 1	< 1	< 1	< 1	< 1	< 1

Aqueous Extract Solution	Unit	GOS-5A		GOS-6A		GOS-7A		GOS-8	GOS-9
		a	b	a	b	a	b		
Sample Description									
Borehole Length	[m]	92.85		103.04		117.38		*cf.* Tab. 7-2	*cf.* Tab7-2
Stratigraphy		Effingen M.		Effingen M.		Effingen M.			
Rock Type		sandy-calcareous marl		sandy-calcareous marl		argillaceous limestone			
Experiment Time	[hours]	24	24	24	24	24	24		
Solid – Liquid Ratio (S:L)		1.000	1.000	1.000	1.000	1.000	1.000		
Conditions		ambient	ambient	ambient	ambient	ambient	ambient		
Sample Temperature	[ºC]	20	20	20	20	20	20		
Fluoride (F^-)	[mg/L	3.2	3.3	4.4	4.5	1.9	1.8		
Chloride (Cl^-)	[mg/L]	94.9	96.5	255.1	253.2	128.4	131.3		
Bromide (Br^-)	[mg/L]	< 0.5	< 0.5	0.8	0.9	< 0.5	< 0.5		
Sulphate (SO_4^{2-})	[mg/L]	468.3	468.9	427.0	421.4	576.1	580.8		
Nitrate (NO_3^-)	[mg/L]	< 1	1.6	< 1	< 1	< 1	1.2		

Tab. 7-1: (continued)

a, b represent duplicate extractions)

Aqueous Extract Solution	Unit	GOS-10A		GOS-11A		GOS-12A	
		a	b	a	b	a	b
Sample Description							
Borehole Length	[m]	133.08		145.59		153.31	
Stratigraphy		Effingen M.		Effingen M.		Effingen M.	
Rock Type		sandy-argillaceous limest.		argillaceous limestone		sandy-calcareous marl	
Experiment Time	[hours]	24	24	24	24	24	24
Solid – Liquid Ratio (S:L)		1.000	1.000	1.000	1.000	1.000	1.000
Conditions		ambient	ambient	ambient	ambient	ambient	ambient
Sample Temperature	[°C]	20	20	20	20	20	20
Fluoride (F^-)	[mg/L]	3.1	3.3	3.0	3.3	3.1	2.9
Chloride (Cl^-)	[mg/L]	180.4	181.6	72.9	71.9	349.9	330.2
Bromide (Br^-)	[mg/L]	0.6	0.7	< 0.5	< 0.5	1.3	1.0
Sulphate (SO_4^{2-})	[mg/L]	331.5	331.4	415.1	413.5	591.0	580.3
Nitrate (NO_3^-)	[mg/L]	1.6	1.5	< 1	1.2	1.0	< 1

Tab. 7-2: Chemical composition of aqueous extract solutions of samples GOS-8 and GOS-9 at different S:L ratios.

a, b represent duplicate extractions.

Aqueous Extract Solution	Unit	GOS-8A		GOS-8B		GOS-8C		GOS-8D	
		a	b	a	b	a	b	a	b
Sample Description									
Borehole Length	[m]	122.89		122.89		122.89		122.89	
Stratigraphy		Effingen M.							
Rock Type		sandy-argillaceous limestone							
Experiment Time	[hours]	24	24	24	24	24	24	24	24
Solid – Liquid Ratio (S:L)		1.000	1.000	0.500	0.501	0.250	0.250	0.101	0.101
Miscellaneous Properties									
Chemical Type		Na-SO_4-Cl-HCO_3	Na-SO_4-Cl-HCO_3	Na-HCO_3-SO_4-Cl	Na-HCO_3-SO_4-Cl	Na-HCO_3-SO_4-Cl	Na-HCO_3-SO_4-Cl	Na-HCO_3-SO_4-(Cl)	Na-HCO_3-SO_4-(Cl)
pH (lab)	[-log(H^+)]	8.92	8.85	9.13	9.11	9.26	9.37	9.50	9.51
Conditions		glove-box	glove-box	glove-box	glove-box	glove-box	glove-box	glove-box	glove-box
Sample Temperature	[°C]	20	20	20	20	20	20	20	20
Cations									
Sodium (Na^+)	[mg/L]	224.9	223.7	136.0	133.9	83.5	82.4	43.4	42.8
Potassium (K^+)	[mg/L]	31.1	31.5	21.3	21.1	15.6	15.4	11.6	11.5
Magnesium (Mg^{2+})	[mg/L]	2.2	2.2	1.0	1.1	< 1	< 1	< 1	< 1
Calcium (Ca^{2+})	[mg/L]	6.9	6.8	3.6	3.5	2.7	2.4	1.9	2.1
Strontium (Sr^{2+})	[mg/L]	< 1	< 1	< 1	< 1	< 1	< 1	< 1	< 1
Anions									
Fluoride (F^-)	[mg/L]	4.0	4.0	3.9	4.0	2.8	2.7	1.3	1.6
Chloride (Cl^-)	[mg/L]	135.4	134.8	68.8	69.2	33.7	33.9	13.2	13.2
Bromide (Br^-)	[mg/L]	< 0.5	0.5	< 0.5	< 0.5	< 0.5	< 0.5	< 0.5	< 0.5
Sulphate (SO_4^{2-})	[mg/L]	211.6	211.4	109.8	109.4	58.2	58.2	23.1	23.1
Nitrate (NO_3^-)	[mg/L]	< 1	< 1	< 1	< 1	< 1	< 1	< 1	< 1
Total Alkalinity	[meq/L]	2.69	2.71	2.33	2.32	1.9	1.89	1.29	1.29
Total Alkalinity as HCO_3	[mg/L]	164.1	165.4	142.2	141.6	115.9	115.3	78.7	78.7
Calculated Properties									
Total dissolved solids	[mg/L]	781	780	487	484	313	311	174	174
Charge Balance	[%]	-0.09	-0.34	-0.32	-0.99	0.19	-0.57	2.29	1.59

Tab. 7-2: (continued)

Aqueous Extract Solution	Unit	GOS-9A		GOS-9B		GOS-9C		GOS-9D	
		a	b	a	b	a	b	a	b
Sample Description									
Borehole Length	[m]	123.71		123.71		123.71		123.71	
Stratigraphy		Effingen M.							
Rock Type		sandy-argillaceous limestone							
Experiment Time	[hours]	24	24	24	24	24	24	24	24
Solid – Liquid Ratio (S:L)		1.001	1.001	0.501	0.501	0.250	0.250	0.100	0.100
Miscellaneous Properties									
Chemical Type		Na-Cl-SO_4-HCO_3	Na-Cl-SO_4-HCO_3	Na-Cl-HCO_3-SO_4	Na-Cl-HCO_3-SO_4	Na-HCO_3-SO_4-Cl	Na-HCO_3-SO_4-Cl	Na-HCO_3-(SO_4)-(Cl)	Na-HCO_3-(SO_4)-(Cl)
pH (lab)	[-log(H^+)]	8.76	8.95	8.96	9.04	9.26	9.16	9.49	9.53
Conditions		glove-box	glove-box	glove-box	glove-box	glove-box	glove-box	glove-box	glove-box
Sample Temperature	[ºC]	20	20	20	20	20	20	20	20
Cations									
Sodium (Na^+)	[mg/L]	260.2	261.4	156.0	151.9	89.7	90.6	52.7	52.4
Potassium (K^+)	[mg/L]	38.4	38.4	24.9	24.6	17.2	17.2	12.4	12.4
Magnesium (Mg^{2+})	[mg/L]	2.6	2.7	1.2	1.1	< 1	< 1	< 1	< 1
Calcium (Ca^{2+})	[mg/L]	7.7	7.9	4.0	3.8	2.2	2.4	2.1	1.8
Strontium (Sr^{2+})	[mg/L]	< 1	< 1	< 1	< 1	< 1	< 1	< 1	< 1
Anions									
Fluoride (F^-)	[mg/L]	5.3	5.0	4.8	4.9	3.6	3.6	2.0	2.3
Chloride (Cl^-)	[mg/L]	189.5	187.2	95.2	93.4	44.1	44.5	18.6	18.9
Bromide (Br^-)	[mg/L]	0.5	0.6	< 0.5	< 0.5	< 0.5	< 0.5	< 0.5	< 0.5
Sulphate (SO_4^{2-})	[mg/L]	237.4	236.3	120.3	119.2	61.6	62.1	25.8	25.9
Nitrate (NO_3^-)	[mg/L]	< 1	< 1	< 1	< 1	< 1	< 1	< 1	< 1
Total Alkalinity	[meq/L]	2.86	2.85	2.57	2.56	2.14	2.14	1.57	1.57
Total Alkalinity as HCO_3	[mg/L]	174.5	173.9	156.8	156.2	130.6	130.6	95.8	95.8
Calculated Parameters									
Total dissolved solids	[mg/L]	917	914	564	555	350	351	210	210
Charge Balance	[%]	-1.99	-1.30	-1.91	-2.77	-3.83	-3.65	0.36	-0.72

Tab. 7-3: Mineral saturation and ion-ion ratios of aqueous extract solutions (average) of samples GOS-8 and GOS-9 at different S:L ratios.

Aqueous Extract Solution	Unit	GOS-8A average	GOS-8B average	GOS-8C average	GOS-8D average	GOS-9A average	GOS-9B average	GOS-9C average	GOS-9D average
Sample Description									
Borehole Length	[m]	122.89	122.89	122.89	122.89	123.71	123.71	123.71	123.71
Stratigraphy		Effingen M.				Effingen M.			
Rock Type		sandy-argillaceous limestone				sandy-argillaceous limestone			
Experiment Time	[hours]	24	24	24	24	24	24	24	24
Solid – Liquid Ratio (S:L)		1.000	0.501	0.250	0.101	1.001	0.501	0.250	0.100
Chemical Type		Na-SO_4-Cl-HCO_3	Na-HCO_3-SO_4-Cl	Na-HCO_3-SO_4-Cl	Na-HCO_3-SO_4-(Cl)	Na-Cl-SO_4-HCO_3	Na-Cl-HCO_3-SO_4	Na-HCO_3-SO_4-Cl	Na-HCO_3-(SO_4)-(Cl)
Calculated with Measured Values									
pH	[-log(H^+)]	8.89	9.22	9.32	9.51	8.86	9.00	9.21	9.51
Total CO_2	[mol/L]	2.570E-03	2.096E-03	1.706E-03	1.115E-03	2.766E-03	2.453E-03	1.928E-03	1.375E-03
log pCO_2		-3.77	-4.19	-4.38	-4.77	-3.71	-3.89	-4.21	-4.68
SI Calcite		0.24	0.24	0.15	0.09	0.28	0.13	0.05	0.11
Calculated at Calcite Equilibrium									
pH	[-log(H^+)]	8.62	8.92	9.12	9.38	8.54	8.84	9.15	9.34
Total CO_2	[mol/L]	2.637E-03	2.192E-03	1.770E-03	1.156E-03	2.846E-03	2.498E-03	1.948E-03	1.435E-03
log pCO_2		-3.48	-3.86	-4.15	-4.60	-3.37	-3.72	-4.14	-4.47
Saturation Index									
Calcite		0.00	0.00	0.00	0.00	0.00	0.00	0.00	0.00
Dolomite		-0.21	-0.27	-	-	-0.19	-0.26	-	-
Dolomite (disordered)		-0.78	-0.84	-	-	-0.76	-0.83	-	-
Fluorite		-0.86	-1.08	-1.49	-2.03	-0.60	-0.86	-1.30	-1.25
Gypsum		-2.33	-2.81	-3.16	-3.58	-2.27	-2.76	-3.20	-3.60
Strontianite		-0.57	-	-	-	-0.71	-	-	-
Celestite		-1.67	-	-	-	-1.75	-	-	-
Ion – Ion Ratios									
Na/Cl	[molar]	2.56	3.02	3.78	5.02	2.14	2.52	3.14	4.32
Br*1000/Cl	[molar]	1.65	-	-	-	1.80	-	-	-
SO_4/Cl	[molar]	0.58	0.59	0.64	0.64	0.46	0.47	0.52	0.51
Ca/SO_4	[molar]	22.37	21.92	14.81	7.42	27.20	27.60	21.69	10.94

8 Advective Displacement Experiment

The pore water extraction experiment by advective displacement was technically successful but was relatively time consuming due to the low hydraulic conductivity, and thus a low flow rate for sampling. The experiment was extended beyond the time required for collecting early pore water samples in order to also obtain constraints on transport properties. The salinity used for the artificial pore water was distinctly higher than that of the in situ pore water. This led to relatively large concentration gradients and mixing effects during the experiment. Pore water extraction was started Nov. 30, 2009, and the experiment was terminated February 2, 2011 (430 days). Collection of the first 5 samples that are most directly relevant for the pore water chemical composition took 42 days. A full analysis and quantitative interpretation of the later data relevant for transport properties will be reported elsewhere.

8.1 Drill core sample GOS-8 and sample preparation

Sample GOS-8 (122.89 m borehole depth) from the Effingen Member is a sandy-argillaceous limestone with a sheet silicate content of 20 %, a quartz content of 10 %, a calcite content of 65 %, a dolomite/ankerite content of 3 %, and a pyrite content of 0.6 % based on total sulfur (*cf.* section 4). The sheet silicates are mostly illite (10 %) and illite/smectite mixed layers (6 %), and minor chlorite (2 %) and kaolinite (3 %). The sample was extremely compact (Fig. 8-1). A very thin calcite-filled vein (< 1 mm width) is perfectly planar and oriented parallel to the cylinder axis across the centre of the core (Fig. 8-1). The vein infill appears dense and is free of visible porosity. It was expected that this feature would unlikely form a hydraulic short cut.

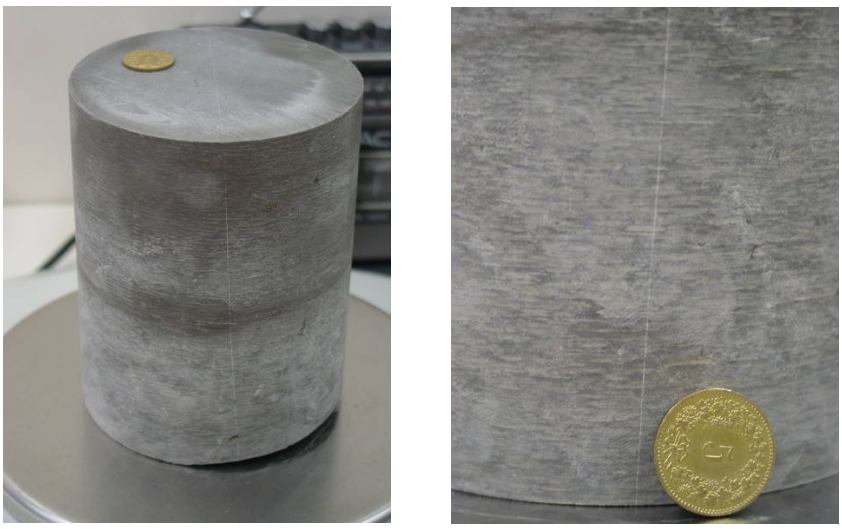

Fig. 8-1: Sample GOS-8 after being cut square just before mounting in the advective displacement apparatus.

There is a very thin calcite-filled vein that is perfectly planar, oriented across the centre and parallel to the cylinder axis (detail on right image). The diameter of the coin is 17 mm. The core diameter is ca. 10 cm.

Accurate cutting of the core was relatively easy due to the excellent core quality. The drill core was cut with a diamond saw using tap water as lubricant. This could not be avoided because the hard and dense rock quality did not allow efficient dry cutting. All outer surfaces of the core

were wrapped tightly in plastic to avoid water contact. The cut surface was blown dry with compressed air immediately after cutting. This minimized exposure of the surface to tap water to one minute or less. It is expected that this will not lead to a measureable contamination. The final dimensions of the core and some other physical properties are listed in Tab. 8-1.

Tab. 8-1: Sample dimensions and measured and calculated physical properties for sample GOS-8.

Sample ID	**Unit**	**GOS-8**
Lithology		sandy argillaceous limestone
Sheet-silicate content	[wt.-%]	total: 20 illite/smectite: 6 illite: 10 smectite: b.d. kaolinite: 4
Core length	[cm]	11.10
Core diameter	[cm]	9.65
Cross-sectional area (calculated)	[cm^2]	73.14
Core volume (calculated)	[cm^3]	811.7
Core mass (water saturated)	[g]	2126.5
Bulk wet density (calculated)	[g/cm^3]	2.62
Water content relative to wet weight (105 °C)	[wt.-%]	2.144
Water mass in core (calculated)	[g]	45.60
Water-loss porosity	[vol.-%]	5.618
Bulk dry density (calculated)	[g/cm^3]	2.564
Grain density (calculated)	[g/cm^3]	2.716

The squared-off cylindrical core sample was mounted between titanium couplings (Fig. 8-2) that connect to an infiltration system when inserted into the pressure vessel. The core is isolated from the confining medium by a layer of Teflon and an outer rubber sleeve. The material transitions between the Teflon, rubber and titanium coupling were additionally sealed with silicon sealant (not in contact with sample, Fig. 8-2) and elastic tape (Fig. 8-3) on the outside to ensure initial tightness when applying the confining pressure.

Teflon discs of 1 mm thickness are placed between the core and the titanium couplings in order to distribute the infiltrating artificial pore water and collect the displaced pore water. An insert of a porous titanium disc with 50 mm diameter and 1 mm thickness was fit into the Teflon disc to prevent a collapse of the porous Teflon when applying large pressures. The completed core assembly is now protected from ambient and can be inserted into the pressure vessel. To do so, the titanium couplings engage into adjustable inserts in the pressure vessel that will adjust exactly to the length of the core assembly (Figs. 8-2, 8-3), and that also seal the capillary tubing that feeds or collects the pore water.

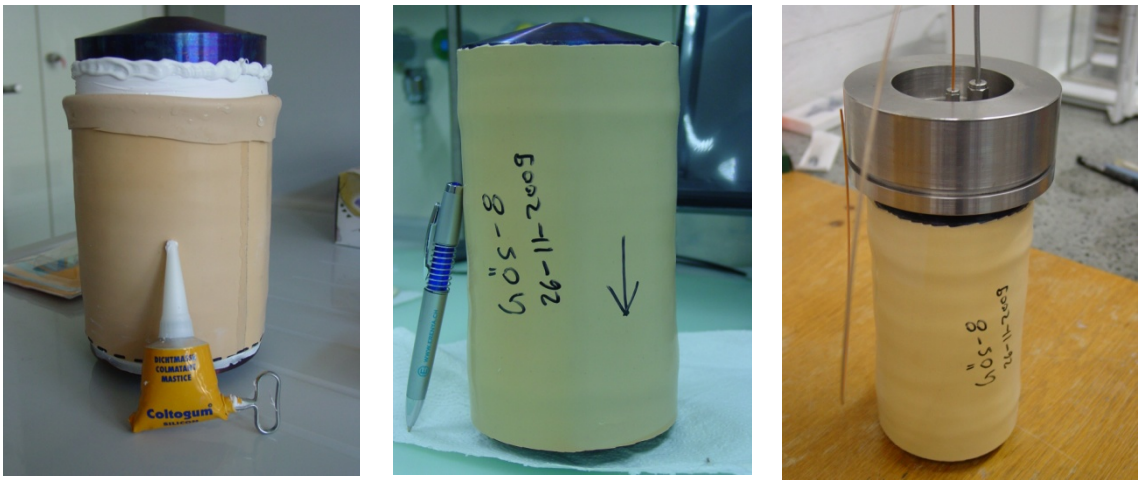

Fig. 8-2: Sample GOS-8 placed between titanium adapters (left), wrapped in Teflon tape and covered with a rubber sleeve applying some silicon sealant at both ends (middle, left) and core assembly with one adjustable insert attached at one end before insertion into the pressure vessel (right).

The titanium is bluish due to heat treatment (corrosion protection by oxide film).

Tubing attached is for the confining medium (right, thicker steel tube) and for the injection of the displacement fluid (thin PEEK capillary).

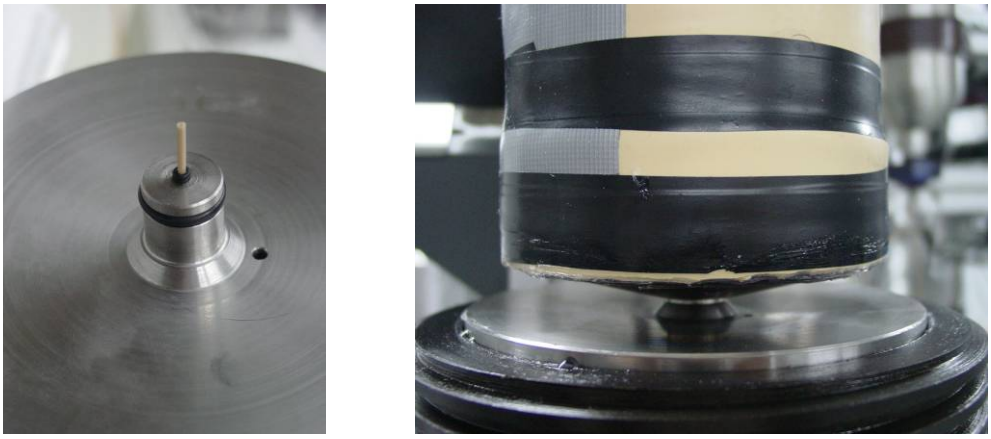

Fig. 8-3: Left: detail of connection of the adapter to the titanium coupling (not shown) with 1/16" PEEK capillary tubing and double O-ring seal; right: assembly being lowered into the pressure vessel.

The lower end of the core assembly is visible with the rubber sleeve reinforced by plastic tape to ensure good initial sealing.

The pressure vessel after inserting the core assembly is shown in Fig. 8-4. The annular space between the core assembly and the pressure vessel inner wall is filled with water and it is vented during the filling procedure. Pressure is applied very slowly in order to ensure good initial sealing against the core. The capillary tubing for inflow and outflow are being left open in order to detect any leakage that would show as expulsion of confining water. Finally, when the con-

fining pressure remained stable over night, all tubing was connected. The inflow is connected to the injection pressure tank via the injection valve, and the outflow is connected via a small-volume flow-through cell for electric conductivity to the sampling syringe (Fig. 8-4).

The infiltration is driven by applying an appropriate helium pressure in the headspace of the injection cylinder. The injection cylinder is made of stainless steel internally coated with a chemically inert polymer (PTFE). Helium is the gas medium of choice because it shows a small solubility and has a solubility that is almost pressure independent – an important issue when operating under large pressure gradients across a sample core.

Electric conductivity was monitored continuously with a data acquisition system. Pressures were very stable and were not monitored, but recorded regularly during routine inspection. Sampling syringes were changed after the desired amounts were collected. The samples were left in the syringes but firmly capped, and stored in a refrigerator before analysis. There were no technical problems during the experiment and all systems performed well.

A water content of 2.33 wt.-% (relative to saturated wet mass) and some other physical properties were measured on samples from the same core sample, and are reported in Tab. 5-1.

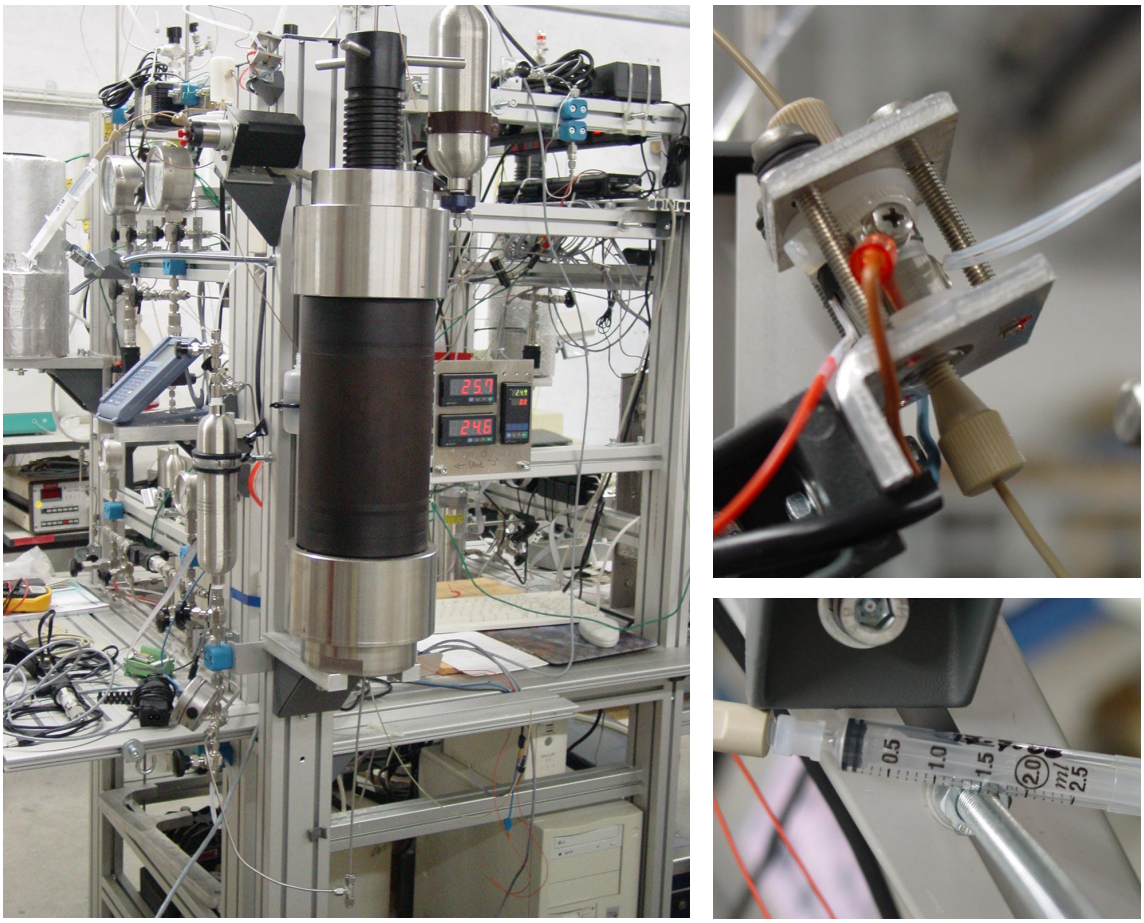

Fig. 8-4: Advective displacement apparatus.

Pressure vessel (left, black steel cylinder). The core assembly located inside is axially confined by the adjustable spindle extending from the top (black, with handle bars). Detail of the small-volume flow-through cell for electric conductivity (top right). Detail of the connection of the outflow to a 2.5 mL sampling syringe (bottom right).

The in-line measurement of pH was performed with a very small flow-through cell and a Ross™ micro combination electrode from Orion (Fig. 8-5). The cell was custom-made in-house and has a dead volume of 20 – 50 µL. pH was measured continuously only during two different time intervals to avoid drift problems, for 29 and 22 hours, respectively. Calibration was performed without removing the electrode with the help of a 6-port stream switching valve that allowed to alternate between measurement mode (pH-cell in-line) and calibration mode (pH-cell connected to calibration port). Calibration solutions were slowly injected with syringes to avoid pressure pulses. Standard solutions with pH values of 4, 7 and 9 were used. Calibration was performed before each measurement period and a calibration check was performed after each period. Electrode drift was negligible. Combined uncertainties from calibration and drift are ca. ± 0.05 pH units.

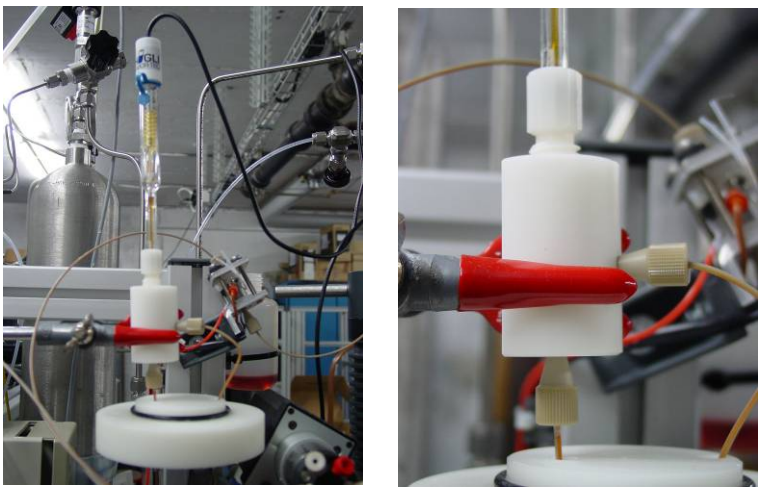

Fig. 8-5: Flow-through cell for in-line measurement of pH with micro-pH electrode.

Materials are POM (white) and PEEK for tubing and fittings (brown).

The diameter of the combination electrode is 3 mm at the front part (not visible) and 6 mm at the shaft above the cell.

8.2 Artificial pore water used for the displacement

The artificial pore water (APW) used for displacement was mixed according to a recipe that was based on preliminary data from aqueous leaching. The more saline variant of two options was used (based on data from OFT-16, Waber 2008a). The nominal composition based on the recipe and the weighed-in chemicals, and measured compositions are given in Tab. 8-2. The APW was traced with 99.99 % pure deuterium to a value of approximately +300 ‰ in δ^2H. The APW used was from the same batch as mixed for the work performed on samples from the borehole in Oftringen (Waber 2008a).

The analytical procedures are detailed in section 8-5. Two samples of the APW were sent to BGS for analysis (samples BGS (1) and BGS (2) in Tab. 8-2). The CO_3-values were calculated from the alkalinity determined by potentiometric titration, and are interpreted as equivalent to the total inorganic carbon content. Carbonate was added as Na-bicarbonate in the recipe. One sample of APW was also analysed at our Institute (Tab. 8-2) confirming the other results.

The APW was modelled based on preliminary data from aqueous extracts of samples OFT-15 and OFT-16. The following assumptions were made for modelling the pore water compositions:

- Cl: Cl concentrations of the extracts were re-calculated assuming a Cl-accessible porosity of 50 % of the water-loss porosity (8.9 and 4.8 vol.-% for OFT-15 and OFT-16, respectively)
- Br: Same assumptions as for Cl
- SO_4: SO_4/Cl ratio of sea water
- TIC: fixed to atmospheric P_{CO2}
- Na: charge balance minus K
- K: Na/K of the aqueous extract
- Ca: equilibrium with calcite
- Mg: equilibrium with dolomite

Tab. 8-2: Composition of the artificial pore water used for displacement.

Component	**Value**	**Value**	**Value**	**Value**	**Value**	**Units**
	Recipe	**Weighed-in**	**Analyzed BGS (1)**	**Analyzed BGS (2)**	**Analyzed Uni BE (1)**	
Na^+	11903	11909	12236	12314	11530	[mg/L]
K^+	835	836	870	872	842	[mg/L]
Ca^{2+}	33.0	33.3	30.5	30.4	37.1	[mg/L]
Mg^{2+}	15.5	15.7	14.4	14.4	< 20	[mg/L]
Cl^-	17705	17716	17298	17335	17375	[mg/L]
SO_4^{2-}	1918	1917	1891	1886	1875	[mg/L]
CO_3^{2-}	162	163	160	162	162	[mg/L]
Charge imbalance	0.0	0.0	2.5	2.72	1.2	[%]
δ^2H (tracer)		ca. +300	+247.8	+248.8		[‰ SMOW]
$\delta^{18}O$ (lab water)			-11.34	-10.34		[‰ SMOW]

Charge imbalance: (cations-|anions|)/(cations+|anions|)*100

8.3 Experimental conditions

The experiment was carried out at room temperature (19 – 24° C). The outflow was connected to a syringe exerting some frictional back pressure (< 0.1 bar) that is negligible compared to the infiltration pressure. The infiltration pressure was initially set to 55.8 bar and decreased gradually to 49.5 bar over 430 days (Fig. 8-6). This gradual decrease is due to the fluid volume continuously pushed out from the pressurized container holding the artificial pore-water through the sample core, and possibly also due to any remaining small helium leakage rate. The confining pressure was set to 72.5 bar and remained constant (Fig. 8-5). The confining pressure is set by a

compressed argon head space in a liquid/gas pressure compensation cylinder connected to the water-filled confining volume of the pressure vessel. The purpose of the compensation cylinder is to dampen pressure changes due to changes in room temperature.

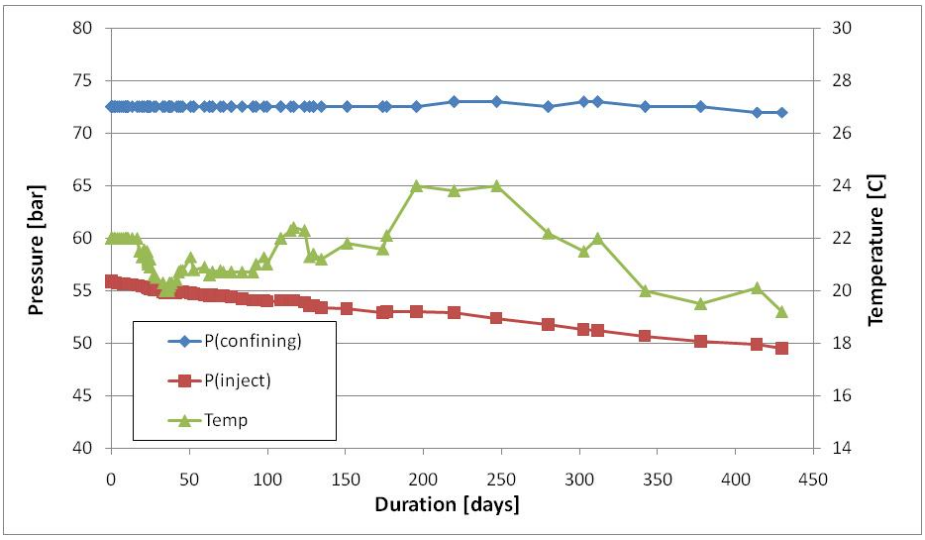

Fig. 8-6: Experimental conditions (pressures, temperature) during the pore water displacement experiment.

8.4 Hydraulic properties

Injection of artificial pore water was started on November 30, 2009, at 22:40. The first drop of displaced pore water reached the syringe on December 7, 2009, after 6.4 days. Before that, only gas from the dead space was expelled, and released from the 1st sampling syringe three times. Syringes with a 2.5 mL capacity were used during the first stage for the first two samples, followed by 5 mL syringes.

There is some gas from the dead space expelled at the beginning of the displacement. This gas can be quantified in the syringe, and is also recorded on-line as periods with almost zero-conductivity when gas bubbles pass through the measuring cell. The amount of gas on the injection side – mainly contained in the porous Teflon and titanium – was removed by applying vacuum prior to injection. The gas contained in the dead space of the extraction side was flushed with argon by a few alternating cycles of moderate vacuum and overpressure. This does not reduce the dead space gas, but reduces the possible contamination by atmospheric components.

The hydraulic conductivity K [m/s] of the sample can be calculated for each sampling interval from the average volumetric flow rate, the sample length, the cross section, and the average difference in hydraulic head applied during displacement, according to equation 8 (section 3.6). This is shown in Fig. 8-7, where the average flow rate is plotted along with the calculated hydraulic conductivity.

The first two samples of 0.38 and 0.44 g were taken after 8.4 and 9.8 days, respectively, but this sampling interval cannot be evaluated in terms of hydraulic conductivity because it comprises the time required to partially fill the dead space with fluid. The third sample taken after 19.7 days corresponds to the first point plotted on Fig. 8-7. This sample and several subsequent

samples are still affected by gas. Sampling gas instead of pore water will results in a low apparent hydraulic conductivity computed from masses of the liquid collected. The proportion of gas involved in sampling is gradually decreasing with time, and in concert, the scatter in the computed hydraulic conductivities becomes smaller.

The hydraulic conductivity becomes constant after ca. 150 days until 250 days. The decrease observed between 250 days and 400 days is not understood. In claystones (Opalinus Clay), a slight and gradually decrease in hydraulic conductivity is observed initially due to some convergence effects subsequent to applying the external confining pressure. Alternatively, chemical precipitation effects may also reduce the hydraulic conductivity. The decrease is relatively minor in absolute terms but well resolved by the data. The measurements are very accurate after the first few samples because all quantities required in equation 11 can be measured to better than 1 % relative.

Presently, the best estimate of the hydraulic conductivity is $1.3 \cdot \times 10^{-13}$ m/s measured between 150 and 250 days.

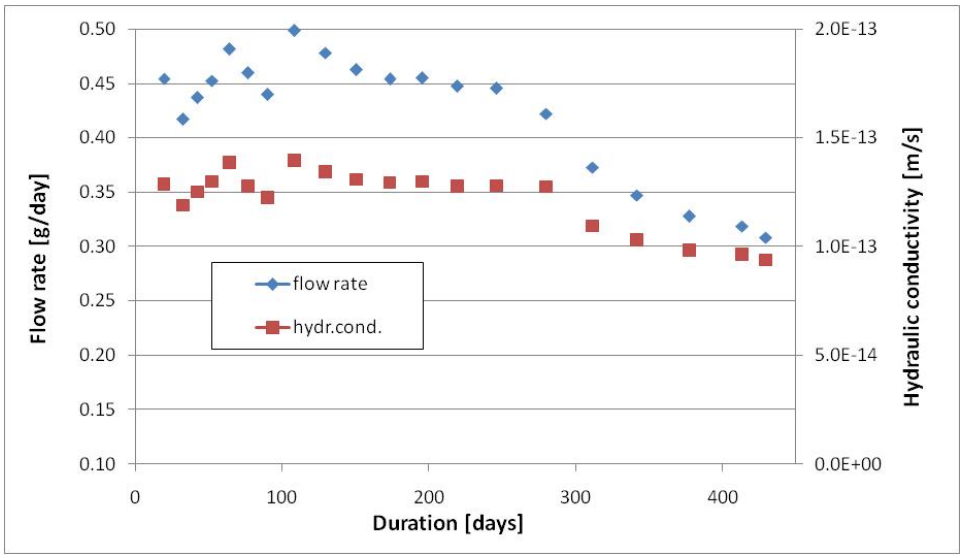

Fig. 8-7: Hydraulic conductivity and average flow rate derived from individual sampling intervals.

8.5 Chemical composition of the extracted aliquots

The electrical conductivity was monitored continuously as a summation parameter that is similar and nearly proportional to ionic strength. A very small conductivity cell from Metrohm was used with an inner diameter of approximately 0.8 mm and a cell constant of 22.7 cm^{-1} that was connected to a Metrohm 712 conductometer. No temperature compensation was performed because of technical difficulties in connecting the very small built-in thermistor. Instead, the readings were recorded manually at regular laboratory checks. The dependence of conductivity on temperature is approximately 2 %/K. The cell and instrument were calibrated with a conductivity standard of ca. 14 mS/cm (at 25 °C).

The electrical conductivity log is shown in Fig. 8-8 along with the temperature. The initial period with only gas transport is seen as a near-zero conductivity. Occasional drops in con-

ductivity mark the passage of a gas bubble through the outflow capillary at the moment of taking a reading. There is an initial relatively steep rise from 20 to 25 mS/cm, a short plateau and a gradual rise to a longer-lasting plateau at 30 mS/cm. The decrease in conductivity after 250 days is initially also a temperature effect. A drop to 20 mS/cm observed after 300 days is most likely a calibration offset. This could be confirmed by a calibration test after the experiment, whereby also after acid cleaning the original performance of the cell could be re-established. The conductivity values may not be true values over extended time periods due to drift associated with such corrosion effects on the electrodes.

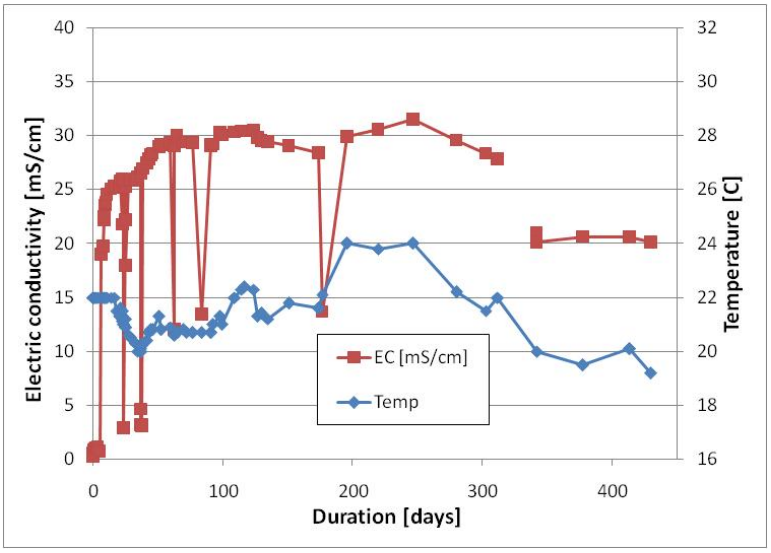

Fig. 8-8: Electric conductivity measured in-line, and room temperature.

A total of 22 samples were taken, containing between 0.38 and 12 ml. Sampling intervals are depicted in Fig. 8-9, where time is also expressed in pore volumes on the left ordinate. Total water content determined by water-loss at 105 °C was used as basis for this conversion of time into pore volume.

The chemical composition of all samples was analyzed in-house. Data is shown for samples #1 to #15, with analytical work still in progress for the later samples. The first 15 samples cover the first 220 days of the experiment. The analytical program and methods are listed in Tab. 8-3. The results of the first 15 samples are listed in Tab. 8-4. The results of the injected artificial pore water are given in Tab. 8-2. The data is displayed in graphical form and discussed in Section 8.6 and Section 8.7. The analyses of the APW by BGS and in-house (Tab. 8-2) were averaged and entered in Tab. 8-4.

The alkalinity was determined by potentiometric titration, and this value was re-calculated as total inorganic carbon (TIC) and also as equivalent bicarbonate (HCO_3^-) in Tab. 8-4. Because of some organic carbon present as low-molecular-weight organic acids visible in ion chromatography, a part of the alkalinity is represent as organic acids, and the re-calculations as TIC or bicarbonate are *equivalent* values and should not be strictly interpreted as true TIC or bicarbonate. The earliest alkalinity was measured in sample #4 and is rather high compared to all subsequent measurements. It is possible, that initially more organic acid was mobilized (oxidation effects?), and that this contributed significantly to this comparatively large alkalinity.

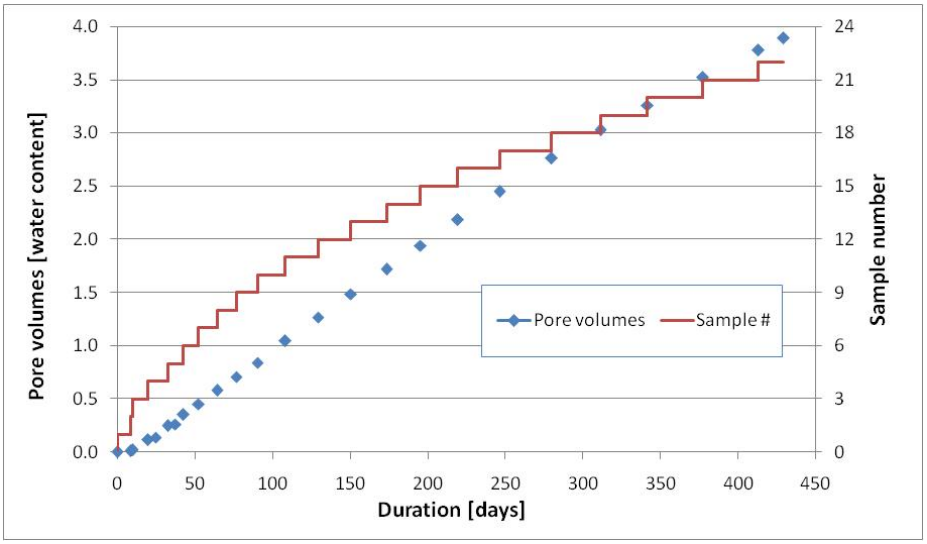

Fig. 8-9: Plot of time intervals for each sample expressed as function of sampling time (abscissa) and pore volume (left ordinate).

Tab. 8-3: Analytical methods used for the analysis of sample aliquots.

Component	**Laboratory**	**Method**
Na, K, Ca, Mg, Sr	Uni Bern	Ion chromatography
F, Cl, Br, NO_3, SO_4,	Uni Bern	Ion chromatography
pH, alkalinity	Uni Bern	Potentiometric titration

The presence of low-molecular-weight organic acids also made the determination of fluoride impossible due to overlapping peaks in the ion chromatogram. Fluoride values are therefore omitted from Tab. 8-4.

Nitrate was measured but was only detected in sample #1 very near detection, but not in all other samples. Nitrate is omitted from Tab. 8-4.

There are three types of pH measurements reported. The initial pH measured for alkalinity titration is listed and pH values that were obtained from measuring a separate aliquot before titration. Two pH values were measured in-line as described above, and these values are marked by an asterisk.

Only incomplete analyses could be obtained from samples #1 and #2 due to their small sample size of only 0.38 and 0.44 ml. It should be noted that the 1st sample recovered may be affected somewhat by contamination and near-surface alteration effects (e.g. oxidation) compared to later samples. But in case of an early admixing of APW, the earliest sample is the closest to the in-situ pore water, as is the case for this experiment.

Tab. 8-4: Chemical composition of sample aliquots and APW (mg/l).

Sample	PV	Na	K	Mg	Ca	Sr	Cl	Br	SO4	alk (meq)	alk (HCO3)	pH (tit)	pH
Gös-1	0.01	5181	104	485	1158	63	8867	34.7	1109				
Gös-2	0.02	5493	104	667	1403	77	9682	36.1	1127				
Gös-3	0.12	5557	103	599	1273	96	11063	35.6	1181				* 6.87
Gös-4	0.25	5792	105	638	1318	83	12204	30.9	1201	6.63	405	7.06	7.22
Gös-5	0.35	6005	110	672	1481	96	12986	33.9	1221				* 7.28
Gös-6	0.45	6351	113	740	1545	105	13767	20.1	1228				
Gös-7	0.58	6552	113	755	1623	103	14349	17.2	1258				
Gös-8	0.71	6841	119	823	1704	103	14917	13.3	1293	2.80	171	7.05	
Gös-9	0.84	6950	123	860	1770	110	15507	11.3	1335	2.50	153	6.94	
Gös-10	1.04	7172	114	829	1842	112	15786	8.7	1489				
Gös-11	1.27									2.03	124	7.40	7.36
Gös-12	1.49	7505	120	880	1862	121	16326	4.2	1536				
Gös-13	1.72	7551	122	850	1806	122	16777	3.1	1601				
Gös-14	1.94									1.93	118	7.37	7.33
Gös-15	2.18	7862	128	822	1842	111	17085	1.6	1709				
APW		12250	870	14.4	30.5	0	17350	0	1880				

PV = pore volumes (at end of sampling interval)
pH (tit) = initial pH during alkalinity titration
* = pH measured in-line during pore water extraction

8.6 Breakthrough of passive tracers as mixing indicators

As a first approximation, the bromide may be considered as a non-reactive tracer that is not present in the APW and, hence, will be gradually flushed out of the sample core. Likewise, chloride may also be used as a non-reactive tracer due to the large difference between the APW and the early extracts. The break-through behaviour of these tracers can be interpreted in terms of mixing indicators of the proportion of APW contained in the extracted sample aliquots. The break-through of bromide and chloride are shown in Fig. 8-10, along with sulphate for compare-son, as an anion that is not expected to behave conservatively.

The mixing factors or break-through fractions ($0 < f < 1$) are computed assuming that the first sample represents the in situ pore water composition, according to:

$$f = (c_{sample} - c_{in\text{-}situ}) / (c_{APW} - c_{in\text{-}situ}) \qquad (10)$$

The break-through curve for bromide is quite different from that for chloride at early times but merges after ca. 1.5 pore volumes. While bromide remains close to constant for the first three samples, chloride is increasing already significantly after the 1st sample. The distinct difference between the two is not understood, as is the apparent immediate break-through of chloride. The apparent outlier in the bromide trend (sample #5) could not be resolved. A nearly full break-through for Br and Cl is expected after approximately two pore volumes.

The relatively fast break-through observed for Cl and Br suggest that there is some anion exclusion effect involved that forces advective anion transport through a reduced cross-sectional area compared to the full water-filled pore space. This will result in a relatively fast average linear pore water velocity compared to bulk water.

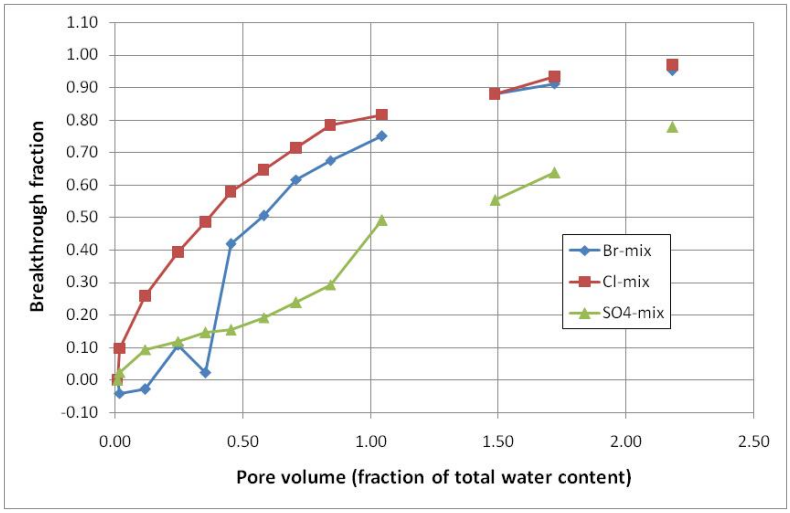

Fig. 8-10: Break-through fraction of anions plotted against pore volumes (relative to total water content) at sampling time.

APW is plotted on the right at a pore volume of 2.2.

The break-through behaviour of sulphate is much slower than that of Br and Cl, and this suggest some reactive process involved that is operating as a retardation factor.

The pending analyses of δ^2H are expected to provide an additional constraint on the mixing extent, although the amounts collected for sample #1 and #2 are insufficient to provide data at very early times. The mixing factors obtained from the break-through of the deuterium water tracer is expected to be different from those obtained from the break-through of anions. If a significant anion-exclusion effect is present, the anion-breakthrough will proceed faster compared to that of a water tracer, and the resulting mixing factors for deuterated water will be larger smaller than those for the anions.

8.7 Discussion of geochemical evolution of eluted pore water samples

The compositional evolution of the extracted pore water vs. pore volume of the major components is shown in Fig. 8-11, and in Fig. 8-12 for minor components. Only the anion components Cl, Br and – to a lesser extent – also SO_4 reach the APW composition after two pore volumes. Cation concentrations differ significantly from the APW composition after two pore volumes. This process is most likely controlled by ion-exchange processes whereby a buffering capacity is present equivalent to the ion exchange capacity of the drill core sample that first has to be displaced before significant changes will become evident in the extracted aliquots. In this case, Na from the APW is being taken up by the exchanger, whereas Ca, Mg and Sr are being released. After flushing with some number of pore volumes, also the cation concentrations are expected to approach the injected APW composition.

The apparent outlier in almost all major component concentrations (Ca, Mg, Na, also Cl) of sample #2 is not understood. The trends defined by later samples would extrapolate relatively smoothly to sample #1, and therefore sample #2 is not considered a reliably sample for the in-situ pore water composition.

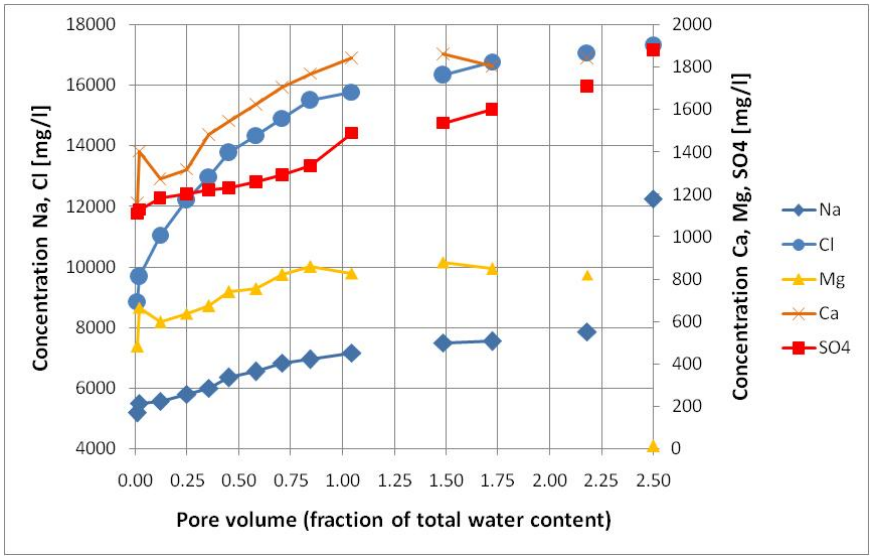

Fig. 8-11: Compositional evolution of major components Na, Cl (left axis), Ca, Mg and SO_4 (right axis) during pore water displacement plotted vs. pore volume at sampling time.

APW is plotted on the right at 2.5 pore volumes (Ca concentration in APW is 31 mg/l but this is off-scale in the plot).

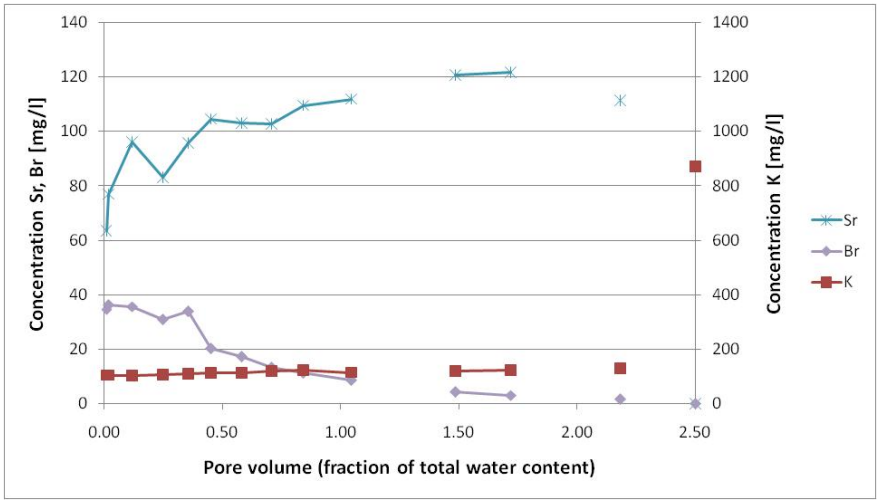

Fig. 8-12: Compositional evolution of minor components Br, Sr (left axis), and K (right axis) during pore water displacement plotted vs. pore volume at sampling time.

APW is plotted on the right at 2.5 pore volumes.

It is concluded that the first sample is likely the best representation of the displaced pore water composition and that this sample is the least affected by admixing of the APW. Unfortunately, this is a very small sample on which only a limited amount of analytics could be performed. Specifically, there is no pH measurement available and no measurement of alkalinity.

9 Constraints on Pore Water Composition

Pore water characteristics of the low-permeability rocks encountered by the Gösgen borehole KB5a were derived by indirect methods based on drillcore material. The derivation of pore water data by various extraction techniques requires the preservation of the drillcore samples in their originally saturated state. Such preservation was only applied to two samples (GOS-8 and GOS-9), whereas all other samples were desaturated and exposed to air for a month before analyses. This puts limitations to the derivation of pore water data, because no reliable information about the *in situ* water- and solute-accessible porosity could be derived for such samples. For the two preserved samples for which porosity data could still be obtained, the derivation of pore water data requires detailed knowledge of the rock composition and a careful evaluation of chemical and isotopic data gathered for potential perturbations induced (e.g. mineral reactions during the experiments and sample treatment in the laboratory etc,).

On samples GOS-8 and GOS-9 that were preserved in their original saturated state pore water was extracted directly from the drillcore by advective displacement (GOS-8) and indirectly by aqueous extraction (GOS-8 and GOS-9). The latter allows estimating the concentration of conservative constituents like chloride and bromide by back-calculating the results of aqueous extraction to the water-content porosity and this hinges on the assumed or inferred ion-specific accessible porosity. Aqueous extraction was also applied to the non-preserved remaining samples. For these even more assumptions had to be made such as the physical porosity determined by bulk dry density measurements to represent the *in situ* physical porosity. As shown in Chapter 5 this is unlikely the case and for these samples the back-calculation of conservative element concentrations bears an even larger uncertainty.

For the Gösgen borehole KB5a reliable pore water data are thus essentially limited to two samples. This precludes a more in depth evaluation of the data in the context of a palaeo-hydrogeological evolution and the present-day boundary conditions of the system (i.e. the groundwater in the aquifers surrounding the low-permeability formation). This is only possible if formation-scale *in situ* pore water concentration profiles could be produced (e.g. Waber 2008a).

9.1 Pore water composition from advective displacement experiment

It was concluded in Section 8 that the first sample aliquot was likely the best representation of the displaced pore water composition and the least affected by admixing of the artificial pore water used for displacement. Unfortunately, with this very small sample only a limited amount of analytics could be performed. Specifically, there is no pH measurement available and no measurement of alkalinity. A best estimate of the in-situ pore water composition is given in Tab. 9-1 along with some comments.

The analytical uncertainties are likely somewhat larger than 5 % due to the relatively large dilution factors applied for ion chromatography necessitated by the small available sample volume. Uncertainties are much larger for alkalinity because of the absence of a measurement for the first aliquot and also due to the presence of an uncertain amount of organic acids (see discussion in Section 8). The pH value is also poorly constrained - this is due to the fact that the first pH of 6.87 measured in-line (sample aliquot #4) is distinctly lower than that of ca. 7.2 – 7.3 measured off-line and also in-line for sample aliquot #5. The Br/Cl ratio of $3.9 \cdot \times 10^{-3}$ mg/mg is slightly higher than that in sea water ($3.5 \cdot \times 10^{-3}$ mg/mg), but similar to the other samples reported (Tab. 7-4).

Tab. 9-1: Approximate chemical composition of in-situ pore water from advective displacement and chloride-accessible porosity proportion (GOS-8, 122.89 m).

Parameter	**Value [mg/l]**	**Comment**
Cl	8870	Sample aliquot #1
Br	35.0	Sample aliquots #1-3
SO_4	1110	Sample aliquot #1
Na	5180	Sample aliquot #1
K	104	Sample aliquots #1-3
Ca	1160	Sample aliquot #1
Mg	485	Sample aliquot #1
Sr	63	Sample aliquot #1
Br/Cl*1000	3.9	mg/mg; sample aliquot #1
Alkalinity (total)	170 – 400	Sample aliquots #4 and #8 (as HCO_3)
pH	6.87 – 7.22	Sample aliquot #4 (in-situ and in lab)
Organic acids	Present	Not quantified
Cl-porosity	0.64	Relative to total water-content porosity

If one assumes that the pore water displaced during the advective displacement corresponds to that accessible to chloride, one can calculate the chloride-accessible porosity directly from the value given in Tab. 9-1 and that obtained from the aqueous leachate of the same sample (Tab. 7-2) without any further assumptions. The same holds true also for bromide, although with larger uncertainties associated with measurements at low concentrations. Because Br was below detection in most of the extracts from sample GOS-8, data for bromide cannot be evaluated. The water-content relative to dry mass is required for the recalculation of aqueous extract concentrations, and this was measured to be 2.39 wt.-% for sample GOS-8 is (Tab. 5-1).

The concentration of Cl derived from the aqueous leachate concentrations in the pore water assuming the entire water-content as chloride-accessible can be calculated according to:

$$c_{PW\_WC} = (c_{aq\text{-}extract} \cdot L) / (WC_{dry} \cdot S) \qquad (11)$$

where c denotes the concentrations (mg/l), WC_{dry} the water content relative to dry mass as fraction, and L/S the liquid-to-solid ratio in mass/mass units. A density correction for the electrolyte solution is neglected for such low concentrations of totals dissolved solids. The anion-accessible porosity proportion (p) can be simply calculated as the ratio of the measured chloride concentration from advective displacement and that calculated according to equation (11):

$$p_{chloride} = c_{adv\text{-}disp} / c_{PW\_WC} = (c_{adv\text{-}disp} / c_{aq\text{-}extract}) \cdot WC_{dry} \cdot (S/L) \qquad (12)$$

The chloride concentrations scaled to total water content (4 samples at different solid/liquid ratios, in duplicate) consistently yield 5470 – 5780 mg/l, or 5640 mg/l on average (Tab. 7-2).

The calculated chloride-accessible porosity proportion is therefore 0.64 or 64 %. Additional data and discussion is included in Section 9.3.

The pore water composition given in Tab. 9-1 was modelled with Phreeqc assuming a minimum pH of 6.87 and a maximum pH of 7.22, and assuming equilibrium with respect to calcite for constraining both alkalinity and P_{CO2} at a given pH and Ca concentration. The results of these calculations are given in Tab. 9-2.

Tab. 9-2: Pore water composition modelled with Phreeqc based on input data from Tab. 9-1, bracketing uncertainty with respect to pH and alkalinity.

Parameter	**Value [mmol/kgw]**	**Value [mmol/kgw]**	**Comment**
pH	6.87	7.22	min. / max.
Temperature (°C)	22	22	Laboratory temperature
Cl	254.6	254.6	
Br	0.446	0.446	
SO_4	11.76	11.76	
Na	229.3	229.3	
K	2.71	2.71	
Ca	29.45	29.45	
Mg	20.30	20.30	
Sr	0.732	0.732	
Alkalinity (total)	2.375	1.070	eq/kgw
TIC	2.769	1.139	
$P(CO_2)$	-1.93	-2.63	log(bar)
Charge imbalance	8.75	8.98	% error
SI(calcite)	0.0	0.0	imposed
SI(celestite)	0.08	0.08	
SI(strontianite)	-0.80	-0.80	
SI(gypsum)	-0.37	-0.37	
SI(dolomite)	-0.03	-0.03	

The charge balance (as %-error) of the input data is close to 9 % with an excess of cation charge. This is not perfect but acceptable due to the small sample size and large dilution factors necessary for the analytical work. Dolomite and celestite are close to or slightly above saturation. The range of alkalinity (2.8-1.1 mmol/kgw carbon) and P_{CO2} ($10^{-1.93}$ – $10^{-2.63}$ bar) bracketed by pH are plausible. The TIC range corresponds to 171 – 67 mg/kgw HCO_3, which is within a range covered by measurements in aliquots sampled at later times (Tab. 8-4), but distinctly lower than a value of 400 mg/l obtained for aliquot #4. The latter may be possibly affected by dissolved organic acids, however.

9.2 Pore water chloride concentration from aqueous extraction

As shown in Chapter 7 chloride from aqueous extracts behaves truly conservative and is therefore representative for the pore water. Similar arguments might also apply for bromide and sulphate. However, bromide concentrations are mainly at or below the detection limit of the applied analytical techniques and its behaviour cannot be conclusively evaluated. Sulphate concentrations extracted under oxygen-free conditions from the two originally saturated samples may have been modified by mineral dissolution reactions. The elution behaviour observed in the advective displacement experiment indicates that sulphate is non-conservative, and the early extracts are nearly at saturation with respect to celestite, for example. Based on the limited data set a conclusive evaluation is not yet possible.

In Chapters 6 and 7 it was further shown that cation concentrations in the leachate solutions are affected by cation exchange processes of the rock samples of the Effingen Member and by mineral dissolution reactions (carbonates, sulphides, fluorite) during aqueous extraction. The chemical type of the extract solutions with SO_4^{2-} and Cl^- as major anions further disables the application of known correction models for the derivation of the *in situ* cation exchange properties. This in turn does not allow a straightforward derivation of a pore water composition from aqueous and Ni-en extraction data by geochemical modelling.

The only reliable pore water data that can be generated from aqueous and Ni-en extraction data of the rock samples from the Gösgen borehole KB5a are pore water chloride concentrations for samples GOS-8 and GOS-9, for which a water content could be measured.

Chloride concentrations at the water-loss porosity are about 5.5 g/kg_{H2O} and 7.2 g/kg_{H2O} for samples GOS-8 and GOS-9, respectively (Tab. 9-2). As shown in the previous section, the advective displacement experiment delivers a pore water chloride concentration of 9 g/kg_{H2O} for sample GOS-8. Comparison of these two values suggests a Cl-accessible porosity in sample GOS-8 of about 0.62. Adopting this Cl-accessible porosity delivers a pore water Cl^- concentration of 11.7 g/kg_{H2O} for sample GOS-9.

The Cl-accessible porosity obtained from advective displacement and aqueous extraction differs significantly from the value that one would obtain from measured water activity and specific surface area of samples GOS-8 and GOS-9 assuming full saturation. Such an estimate would yield a proportion of free water of only 0.17 and 0.23. As discussed in Chapter 5, these estimates bear a large uncertainty and are not thought to be reliable. Nevertheless, such low proportions of free water would be consistent with the observations made for the Effingen Member rocks from the EWS-borehole Oftringen, for which an average proportion of free water of 0.22 ± 0.07 was obtained from measured water activity and specific surface area (Koroleva & Mazurek 2008). Interestingly, for the one examined Oftringen sample the comparison of Cl^- concentrations obtained from advective displacement and aqueous extraction delivered a similar Cl-accessbile porosity of only 0.25 (Waber 2008a). These apparent discrepancies between the two sampling sites are currently not understood.

For the samples that were not preserved on site in their saturated state, an estimate of Cl concentrations can be made based on the physical porosity calculated from density measurements (Tab. 9-3). As outlined in Chapter 5, the bulk dry density measurements on these rocks are attached with a large uncertainty due to shrinkage of the rock material during drying. Therefore and combined with the uncertainty associated with the Cl-accessible porosity such estimates have to be regarded as semi-quantitative at the most. Nevertheless and assuming that the perturbbation of the bulk dry density is similar in all samples because of the similar clay content, some information about the spatial distribution of Cl^- in the pore water may be evident. This is because the difference between total (or water-loss) porosity and the Cl-accessible

porosity is essentially a scaling factor for calculating to the true Cl^- concentration from that measured in the aqueous extracts. The distribution with depth of the so derived Cl^- concentration is shown in Fig. 9-2 together with the Cl^- concentrations obtained from aqueous extractions and advective displacement. Note that this approach of using a uniform accessible porosity fraction for chloride is overly simplistic in view of the rather large range of clay contents across this section of the Effingen Member.

For samples GOS-8 and GOS-9, the Cl^- concentrations based on the scaled water-loss porosity are only about 65 % and 83 % of the Cl^- concentration measured in rocks from the EWS-borehole Oftringen (about 14 g/kg_{H2O}) sampled at the same distance from the top of the Effingen Member. The lower Cl^- concentrations seem to be consistent with the shallower occurrence of the Effingen Member at Gösgen and possibly more active hydraulic conditions at the upper boundary of these low-permeability rocks. However, no groundwater data exist from this upper boundary and no further conclusions can be drawn from this observation.

Tab. 9-3: Chloride concentrations from aqueous extraction tests back-calculated to measured water-loss porosity (WL-P) and 62 % water-loss porosity for samples GOS-8 and GOS-9 and the Cl concentration from the advective displacement experiment of sample GOS-8.

Also given are the semi-quantitative estimates of Cl concentrations calculated from 62 % Cl-accessible physical porosity, which was derived from perturbed bulk dry density measurements (data from Tab. 5-1).

Sample	**Depth** [m along borehole]	**Stratigraphy**	**Cl at WL-P** [mg/kg_{H2O}]	**Cl from advective displacement** [mg/L]	**Cl at 0.62 × WL-P** [mg/kg_{H2O}]	**Cl at 0.62 × physical porosity from bulk dry density** [mg/kg_{H2O}]
GOS-1	50.12	Olten M.				*1086*
GOS-2	63.92	Geissberg M.				*4197*
GOS-3	72.77	Effingen M.				*4313*
GOS-4	83.21	Effingen M.				*6658*
GOS-5	92.85	Effingen M.				*6935*
GOS-6	103.04	Effingen M.				*10234*
GOS-7	117.38	Effingen M.				*15855*
GOS-8	122.89	Effingen M.	5659	8870	9128	*7949*
GOS-9	123.71	Effingen M.	7254		11699	*11346*
GOS-10	133.08	Effingen M.				*11108*
GOS-11	145.59	Effingen M.				*11244*
GOS-12	153.31	Effingen M.				*15352*

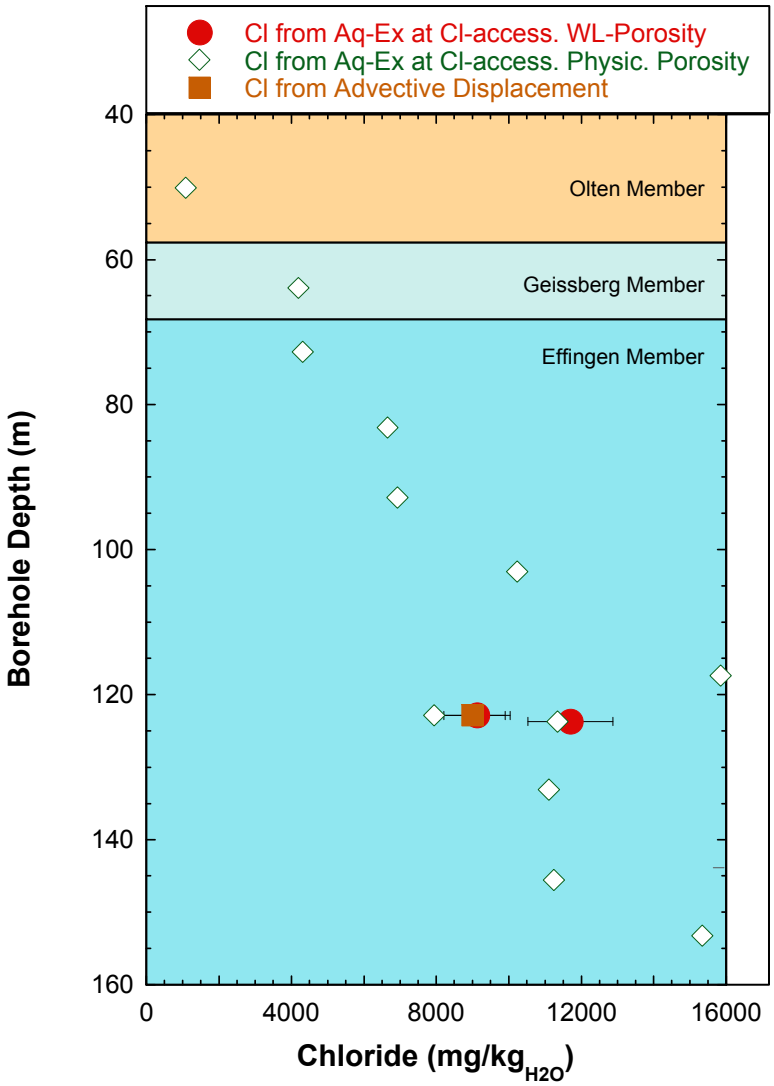

Fig. 9-1: Depth profiles for chlorinity based on scaled chloride concentrations measured in the aqueous extracts assuming 62 % accessible water-loss porosity for samples GOS-8 and GOS-9 in comparison with the Cl concentration from the advective displacement experiment.

Also shown are the semi-quantitative estimates of Cl concentrations calculated from 62 % Cl-accessible physical porosity, which was derived from perturbed bulk dry density measurements.

Red circles: Cl at 0.62 WL-P of samples GOS-8 and GOS-9; brown square: Cl of advective displacement; open diamonds: semi-quantitative Cl at 0.62 physical porosity.

10 Summary and Conclusions

From the Gösgen borehole KB5a 12 samples have been investigated for their pore water characteristics with 10 samples being located in the upper part of the Effingen Member between about 73 and 153 m below surface. Only 2 of the samples have undergone on site conditioning to preserve their saturated state. The remaining drillcore samples were stored unprotected for a few months before the laboratory treatment.

The rocks from the Effingen Member at Gösgen classify as sandy-calcareous marls to argillaceous limestones with variable sand components (quartz and feldspars). The contents of calcite range from 32 wt.-% to 85 wt.-%, quartz from 3 wt.-% to 17 wt.-% and the clay fraction from 10 wt.-% to 34 wt.-%. Dolomite is present in minor amounts of less than 5 wt.-% in most samples. Pyrite is present in all samples at highly variable contents between 0.2 wt.-% and 1.9 wt.-%. The mineralogy of the clay fraction (< 2 µm) is made of illite (5 – 18 wt.-%), illite-smectite mixed layers (4 – 12 wt.-%, kaolinite (< 1 – 4 wt.-%) and sporadically some traces of chlorite.

Whereas the whole rock mineralogy compares well with that of the Effingen Member rocks examined in the EWS-borehole Oftringen, there are some distinct compositional differences in the clay fraction. The Effingen Member rocks at Gösgen have an illite to illite-smectite mixed layers ratio of 1.5 ± 0.4 (n = 10) compared to a ratio of 0.7 ± 0.2 (n = 19) in the clay fraction of the Oftringen samples (De Haller & Mazurek 2008). Furthermore, the rocks at Gösgen have about three times lower contents of kaolinite compared to the Oftringen rocks (2.4 wt.-% compared to 7.6 wt.-% on average) and smectite is absent. These differences might be related to a different diagenetic history although it is somehow counterintuitive to the present-day occurrence of the Effingen Member at Gösgen and Oftringen. A higher maturity of the clay fraction would be expected in the deeper seated Oftringen rocks compared to what is observed.

The gravimetric water content obtained for the two on-site conditioned samples GOS-8 and GOS-9 is 2.33 wt.-% and 2.53 wt.-% (relative to wet mass) and falls within the range given by the Oftringen samples (0.7 – 4.19 wt.-%). Comparable for all samples are the grain density values obtained for the Effingen Member rocks at Gösgen 2.68 – 2.80 g/cm^3) and at Oftringen (2.73 – 2.81 g/cm^3). Differences exist, however, in the bulk dry density, which was measured on dried samples from the Gösgen borehole (2.37 – 2.60 g/cm^3), but calculated from the measured wet density for samples from the Oftringen borehole (2.45 – 2.63 g/cm^3). It appears that the Gösgen samples suffered from shrinkage during drying, which depends on the rock sample's mineralogy and texture and this resulted in too low a bulk dry density. The resulting calculated physical porosity is therefore only semi-quantitative and is associated with a non-systematic, large uncertainty and it is not recommended for the calculation of pore water concentrations.

The range obtained for the specific surface area and its correlation with the clay content compare well between the Effingen Member rocks from Gösgen (specific surface area: 10 – 32 m^2/g) and Oftringen (specific surface area: 2 – 29 m^2/g). Also comparable is the water activity measured on the samples GOS-8 and GOS-9 from Gösgen (a_w = 0.85 and 0.87) with that measured on samples from Oftringen (a_w = 0.81 – 0.93). For both sites this results in a calculated low proportion of free water being 0.17 and 0.23 for the Gösgen samples and between 0.13 – 0.38 for the Oftringen rocks. The reason for such low proportions of free water in the rocks of the Effingen Member is currently not understood. In the case of the Gösgen rocks such a low proportion is inconsistent with the chloride-accessible porosity obtained from the comparison of aqueous extraction and advective displacement data.

Similar as for the Effingen Member rocks from Oftringen only the total cation exchange capacity, CEC, could be determined with some confidence, but not the selectivity for individual cations. The CEC was estimated from the Ni-consumption during the Ni-en extraction tests and varies for samples GOS-8 and GOS-9 between 45 – 56 meq/kg_{rock}. These values compare well with those of Effingen Member rocks from Oftringen with similar total clay contents. As for the Oftringen rocks, the derivation of the *in situ* cation population and exchange selectivity coefficients is hindered by the presence of two equally dominant anions (SO_4^{2-} and Cl^-) in the aqueous extract solution and the absence of an accurate correction method for such a situation.

The aqueous extract solutions at a solid:liquid ratio of 1:1 of samples GOS-8 and GOS-9 contain about 780 mg/L and 915 mg/L dissolved solids and fall within the range given by the Oftringen samples (590 – 1100 mg/L). Similarly, the Gösgen samples are of a general Na-SO_4-Cl-HCO_3 type with SO_4^{2-} and Cl^- being about equally abundant. In these two samples Cl^- behaves chemically conservative. Also SO_4^{2-} appears to behave in a conservative way as indicated by the trends in aqueous extract concentration vs. solid:liquid ratio and calculations of saturation state. Pyrite oxidation did not occur to a significant extent under the applied oxygen-free conditions and no sulphate mineral source seems to have contributed to the SO_4^{2-} inventory in the extract solutions. In contrast, samples prepared under ambient conditions show a significant contribution from pyrite oxidation. The comparison of differently prepared samples from the Gösgen borehole and the similarity of the Effingen Member rocks at the two sites might thus also shed some light on open questions that remained for the aqueous extraction data of the Oftringen rocks.

In the aqueous extract solutions of samples GOS-8 and GOS-9, the concentrations of K^+ (31 – 38 mg/L at S:L = 1) are much higher than in the solutions from the Oftringen rocks (9 – 24 mg/L). The differences are related to the differences in the clay composition of the rocks, i.e. mainly the ratio of illite to illite/smectite mixed layers, and reflect the importance of cation exchange reactions during extraction. It further highlights the necessity of elaborating adequate cation exchange properties for the calculation of a complete chemical pore water composition.

Similarly as for K^+, the concentrations of Na^+ and the alkaline earth elements (Ca^{2+}, Mg^{2+}, Sr^{2+}) in the aqueous extracts were modified by ion-exchange processes and carbonate dissolution and are, therefore, not representative of the pore water.

An advective displacement experiment yielded 22 small sample aliquots over 430 days. The analysed compositions of the first 15 sample are reported here. The artificial pore water (APW) used for the displacement was of a distinctly higher salinity compared to the early extracted aliquots. This resulted in a relatively fast break-through of APW seen as admixture in subsequent aliquots. The anion exclusion effect is evident in the breakthrough behaviour of Cl and Br, but SO_4 is showing some retardation due to mineral/pore water interaction. The first very small sample aliquot appears to be the best approximation for the "free" pore water composition. It has a Cl content of 8.9 g/kg, a sulphate content of 1.1 g/kg, a Na content of 5.2 g/kg and a Ca content of 1.2 g/kg (Table 9-1 for full data set). Alkalinity and pH could not be measured on this very small sample. pH is loosely constrained between 6.9 and 7.2, and alkalinity and P_{CO2} ($10^{-1.9}$ – $10^{-2.6}$ bar) were modelled with Phreeqc at assumed calcite saturation (Tab. 9-2), with plausible overall results. A chloride-accessible porosity proportion of 0.64 was calculated from the concentrations in the first sample aliquot and the chloride content obtained from aqueous leaching.

11 Referenzverzeichnis

Albert, W. & Bläsi, H.R. (2008): NOK EWS-Bohrung Oftringen: Geologische, mineralogische und bohrlochgeophysikalische Untersuchungen (Rohdatenbericht). Nagra Arbeitsbericht NAB 08-02. Nagra, Wettingen, Switzerland.

Albert, W., Bläsi, H.R. & Weber, H.P. (2009): Geologische und geophysikalische Untersuchungen in Bohrungen am Standort Gösgen/Niederamt. Unpubl. Nagra Project Report. Nagra, Wettingen, Switzerland.

Baeyens, B. & Bradbury, M.H. (1994): A Physico-Chemical Characterisation and Calculated *in situ* Porewater Chemistries for a Low Permeability Palfris Marl Sample from Wellenberg. Nagra Tech. Report NTB 94-22. Nagra, Wettingen, Switzerland.

Bradbury, M.H. & Baeyens, B. (1997/98): Derivation of *In situ* Opalinus Clay Porewater Compositions from Experimental and Geochemical Modelling Studies with Corrigendum. Nagra Tech. Report 97-07. Nagra, Wettingen, Switzerland.

Brunauer, S, Emmett, P.H. & Teller, E. (1938): Adsorption of gases in multimolecular layers. J. Amer. Chem. Soc. 60, 309-319.

Enachescu, C., Rohs, S. & Böhner, J. (2010): Borehole Gösgen SB2 – Hydraulic Packer Testing. Unpubl. Nagra Project Report. Nagra, Wettingen, Switzerland.

Feller, C., Schouller, E., Thomas, F., Rouiller, J. & Herbillon, A.J. (1992): N2-BET specific surface areas of some low activity clay soils and their relationships with secondary constituents and organic matter contents. Soil Science 153, 293-299.

Fisch, H.R., Rösli, U., Reinhardt, S., Yeatman, B., Senger, R. & Dale, T. (2008): Oftringen borehole – Hydraulic packer testing. Nagra Arbeitsbericht NAB 08-15. Nagra, Wettingen, Switzerland.

Füchtbauer, H. (Ed.) (1988): Sedimente und Sedimentgesteine. Schweizerbart, Stuttgart, 1141 p.

De Haller, A. & Mazurek, M. (2008): Rock Mineralogy. Chapter 4 in Waber, H.N. (ed.): Borehole Oftringen: Mineralogy, Porosimetry, Geochemistry, Pore Water Chemistry. Nagra Arbeitsbericht NAB 08-18. Nagra, Wettingen, Switzerland.

Hobbs, M.Y., De Haller, A., Mäder, U., Meier, D. & Koroleva, M. (2010): Borehole DGR-3 and DGR-4 porewater investigations. Unpubl. Intera Technical Report. Intera, Ottawa, Canada.

Koroleva, M. & Mazurek, M. (2008): Petrophysical Properties. Chapter 7 in Waber, H.N. (ed.): Borehole Oftringen: Mineralogy, Porosimetry, Geochemistry, Pore Water Chemistry. Nagra Arbeitsbericht NAB 08-18. Nagra, Wettingen, Switzerland.

Laws, S. & Deplazes, G. (2007): Geologie und Hydrogeologie der Effinger Schichten im Tafeljura und am Jurasüdfuss. Zusammenfassung des Wissensstandes vor den Untersuchungen in den EWS-Bohrungen Küttigen 1, Küttigen 2 und Oftringen. Nagra Arbeitsbericht NAB 07-28. Nagra, Wettingen, Switzerland.

Mäder, U.K. (2006): Porewater chemistry, porosity and hydraulic conductivity of Callovo-Oxfordian claystone at the EST-322 deep drilling site sampled by the method of advective displacement (Laboratoire de Rechereche Souterrain de Meuse / Haute-Marne). Nagra Arbeitsbericht NAB 05-04. Nagra, Wettingen, Switzerland.

Mäder, U.K., Waber, H.N. & Gautschi, A. (2004): New method for porewater extraction from claystone and determination of transport properties with results for Opalinus Clay (Switzerland). *In*: Wanty, R.B. & Seal II, R.R. (eds.): Proc. 11th Internat. Symp. Water-Rock Interaction (WRI-11), Saratoga Springs (N.Y.). Balkema, 445-448.

Mazurek, M., Meier, D. & Müller, H. (2010): WS-H experiment: Geological, petrophysical and geochemical characterisation of drillcores from borehole BHG-B11. Unpubl. Mont Terri Technical Note. Mont Terri Consortium, St. Ursanne, Switzerland.

Müller, W.H., Naef, H. & Graf, H.R. (2002): Geologische Entwicklung der Nordschweiz, Neotektonik und Langzeitszenarien Zürcher Weinland. Nagra Tech. Report NTB 99-08. Nagra, Wettingen, Switzerland.

Nagra (1988): Sedimentstudie – Zwischenbericht 1988. Möglichkeiten zur Endlagerung langlebiger radioaktiver Abfälle in den Sedimenten der Schweiz. Nagra Tech. Report NTB 88-25. Nagra, Wettingen, Switzerland.

Nagra (2008): Vorschlag geologischer Standortgebiete für das SMA- und das HAA-Lager. Geologische Grundlagen. Nagra Tech. Ber. NTB 08-04.

Norton, D. & Knapp, R. (1977): Transport phenomena in hydrothermal systems: The nature of porosity. Amer. J. Sci. 277, 913–936.

Waber, H.N., Gaucher, E.C., Fernandez, A.M. & Bath, A. (2003): Aqueous Leachates and Cation Exchange Properties of Mont Terri Claystones. *In:* Pearson, F.J. et al.: Mont Terri Project – Geochemistry of Water in the Opalinus Clay Formation at the Mont Terri Rock Laboratory. Bern, Switzerland, Federal Office of Water and Geology (FOWG). Geology Series No. 5, 200-237.

Waber, H.N. (ed.) (2008a): Borehole Oftringen: Mineralogy, Porosimetry, Geochemistry, Pore Water Chemistry. Nagra Arbeitsbericht NAB 08-18. Nagra, Wettingen, Switzerland.

Waber, H.N. (2008b): Cation Exchange Properties. Chapter 8 in Waber, H.N. (ed.): Borehole Oftringen: Mineralogy, Porosimetry, Geochemistry, Pore Water Chemistry. Nagra Arbeitsbericht NAB 08-18. Nagra, Wettingen, Switzerland.

Waber, H.N. (2008c): Aqueous Extraction. Chapter 9 in Waber, H.N. (ed.): Borehole Oftringen: Mineralogy, Porosimetry, Geochemistry, Pore Water Chemistry. Nagra Arbeitsbericht NAB 08-18. Nagra, Wettingen, Switzerland.

Appendix A: Chemical and Isotopic Composition of the Groundwater from Packer Test Number 1 in Borehole Gösgen SB2

Analysis was carried out by Hydroisotop GmbH (D-Schweitenkirchen). The tested interval ranges from the Birmenstorf Member to the Hauptrogenstein Formation.

Labor-Nr.		200224
Entnahmestelle		Gösgen SB 2 (216,9-347,0m)
Aquifer		Hauptrogenstein
Laboreingang		03.02.2009
Angabe AG		
pH-Wert vor-Ort		7.7
spez. el. Leitfähigkeit vor-Ort	µS/cm	15700
Sensorik		
Aussehen		leichter, flockiger Niederschlag
Farbe		grau
phys.-chem. Parameter		
spez. el. Leitfähigkeit (25°C) Labor	µS/cm	18050
pH-Wert (20°C) Labor		7.11
Sk-Wert (pH 4,3) Labor	mmol/l	5.28
Bk-Wert (pH 8,2)	mmol/l	1.03
Hauptionen		
Natrium (Na+)	mg/l	3150
Kalium (K+)	mg/l	72.1
Calcium (Ca2+)	mg/l	406
Magnesium (Mg2+)	mg/l	246
Ammonium (NH4+)	mg/l	6.5
Hydrogenkarbonat (HCO3-)	mg/l	322
Carbonat (CO32-)	mg/l	< 3
Chlorid (Cl-)	mg/l	5640
Sulfat (SO42-)	mg/l	617
Nitrat (NO3-)	mg/l	2.7
Nitrit (NO2-)	mg/l	0.31
Bromid (Br-)	mg/l	20,7 / 27
Fluorid (F-)	mg/l	2.27
Iodid (I-)	mg/l	(9)
Spurengehalte		
Lithium (Li+)	mg/l	1.21
Rubidium (Rb+)	mg/l	0.058
Strontium (Sr2+)	mg/l	42
Barium (Ba2+)	mg/l	0.08
Mangan ges.	mg/l	0.073
Eisen ges.	mg/l	0.03
Arsen ges.	mg/l	0.002
Aluminium (Al)	mg/l	0.029
Phosphor ges. (P)	mg/l	0.029
Undissoziierte Bestandteile		
Kieselsäure (H2SiO3) direkt	mg/l	16
Kieselsäure (H2SiO3) Membranfiltrie	mg/l	12
Borsäure (H3BO3)	mg/l	31
meta-Borsäure (HBO2)	mg/l	22
Summenparameter		
Trockenrückstand 110 °C	mg/L	11.2
Trockenrückstand 180 °C	mg/L	10.6
Glührückstand 600 °C	mg/L	9.63
DOC	mg/L	1.55
TOC	mg/L	1.63
Isotope		
Tritium (3H)	TU	0,8 ± 0,57
Sauerstoff-18 (d18O-H2O)	‰	-5.63
Deuterium (d2H-H2O)	‰	-51
Kohlenstoff-14 (14C-DIC)	%-modern	6,58 ± 0,16
Kohlenstoff-13 (d13C-DIC)	‰	-4.2
Schwefel-34 (d34S-SO4)	‰	40.3
Sauerstoff-18 (d18O-SO4)	‰	18.9
Strontium (87Sr/86Sr)		0,707381±0,000018